Distribution Agreement

In presenting this thesis or dissertation as a partial fulfillment of the requirements for an advanced degree from Emory University, I hereby grant to Emory University and its agents the non-exclusive license to archive, make accessible, and display my thesis or dissertation in whole or in part in all forms of media, now or hereafter known, including display on the world wide web. I understand that I may select some access restrictions as part of the online submission of this thesis or dissertation. I retain all ownership rights to the copyright of the thesis or dissertation. I also retain the right to use in future works (such as articles or books) all or part of this thesis or dissertation.

Signature:

_____ _____

Sarah K. Wise, M.D. Date

Wound Healing in Sinonasal Mucosa: Influence of Th2 Inflammatory Mediators

By

Sarah K. Wise, M.D.
Master of Science

Clinical Research

_____
Asma Nusrat, M.D.
Advisor

_____
Charles A. Parkos, M.D., Ph.D.
Advisor

_____
Christine Kempton, M.D., M.Sc.
Committee Member

_____
Amita Manatunga, Ph.D.
Committee Member

Accepted:

_____
Lisa A. Tedesco, Ph.D.
Dean of the James T. Laney School of Graduate Studies

_____
Date

Wound Healing in Sinonasal Mucosa: Influence of Th2 Inflammatory Mediators

By

Sarah K. Wise
M.D., University of Texas Health Science Center, 2001

Advisor: Asma Nusrat, M.D.

Advisor: Charles A. Parkos, M.D., Ph.D.

An abstract of
A thesis submitted to the Faculty of the
James T. Laney School of Graduate Studies of Emory University
in partial fulfillment of the requirements for the degree of
Master of Science
in Clinical Research
2012

ABSTRACT

Wound Healing in Sinonasal Mucosa: Influence of Th2 Inflammatory Mediators

By Sarah K. Wise, M.D.

Background: Inflammatory rhinosinusitis affects over 29 million U.S. adults. Prolonged healing and persistent inflammation following surgery for rhinosinusitis impact quality of life and healthcare resources. Chronic rhinosinusitis (CRS) is categorized as Th1, classically infectious, or Th2, classically allergic with elevated interleukins (IL)-4, 5, and 13. Prior studies demonstrate decreased wound healing with Th2 inflammatory mediator exposure, but this is not extensively studied in sinonasal epithelium.

Hypothesis: Exposure of sinonasal epithelial cell layers *in vitro* to characteristic Th2 inflammatory cytokines IL-4, IL-5, and IL-13 (separately) will impair wound healing rates and decrease expression of specifically-chosen epithelial migratory and intercellular adherens junction proteins compared to control sinonasal epithelial wounds not exposed to cytokines.

Methods: Following 24-hour exposure to IL-4, 5, or 13 versus controls, sterile linear mechanical wounds were created in primary sinonasal epithelial cultures (n = 12 wounds per condition). Wounds were followed for 36 hours or until complete closure and wound areas calculated by image analysis. Group differences in epithelial migratory proteins annexin 2, vinculin, and β1-inegrin and adherens junction proteins E-cadherin and β-catenin were assessed by immunofluorescence labeling, confocal microscopy, and Western immunoblots. Baseline epithelial protein differences by CRS disease state were ruled out by immunofluorescence and Western immunoblots.

Results: Significant wound closure differences were identified across cytokine exposure groups ($p<0.001$). A significant time-group interaction in wound closure was demonstrated by repeated measures ANOVA ($p<0.001$). At 36-hours, 75% of wounds exposed to IL-4 were incompletely closed, whereas 25% of control wounds remained open. With IL-4 exposure, annexin 2 and vinculin at wound edges were decreased versus no-cytokine exposure control ($p<0.01$).

Conclusions: Th2 cytokine IL-4 decreases sinonasal epithelial wound closure *in vitro*. Wound edge migratory proteins are diminished with IL-4 exposure. This supports the hypothesis that Th2 exposure impairs sinonasal epithelial wound healing.

Wound Healing in Sinonasal Mucosa: Influence of Th2 Inflammatory Mediators

By

Sarah K. Wise
M.D., University of Texas Health Science Center, 2001

Advisor: Asma Nusrat, M.D.

Advisor: Charles A. Parkos, M.D., Ph.D.

A thesis submitted to the Faculty of the
James T. Laney School of Graduate Studies of Emory University
in partial fulfillment of the requirements for the degree of
Master of Science
in Clinical Research
2012

ACKNOWLEDGEMENTS

Elizabeth K. Hoddeson, M.D. and Kyle A. DenBeste are graciously acknowledged for their assistance in the performance of laboratory experiments described herein.

Susan Voss, Ph.D. and Ryan Mulligan are acknowledged for their assistance in establishing and maintaining primary sinonasal epithelial cell cultures.

Justin C. Wise, Ph.D. is kindly acknowledged for his assistance in experimental design and statistical analysis.

John M. DelGaudio, M.D. is acknowledged for his clinical mentorship and donation of sinonasal surgical tissue specimens for these studies.

The Robert P. Apkarian Integrated Electron Microscopy Core of the Emory University School of Medicine and its staff are acknowledged for their assistance in obtaining the electron microscopy images presented in this thesis.

This work was supported in part by the following funding sources:

1. Clinical and Translational Science Award Program, National Institutes of Health, National Center for Research Resources KL2 RR0025009 and UL1 RR025008 (S.K.W.)
2. American Rhinologic Society New Investigator Award (S.K.W.)
3. Structure function studies in intestinal epithelial JAM, National Institutes of Health, National Institute of Diabetes and Digestive and Kidney Diseases DK061379 (C.A.P.)

4. Neutrophil interactions with intestinal epithelial cells, National Institutes of Health, National Institute of Diabetes and Digestive and Kidney Diseases, DK072564 (C.A.P.)
5. Intestinal epithelial tight junction structure-function, National Institutes of Health, National Institute of Diabetes and Digestive and Kidney Diseases, DK059888 (A.N.)

TABLE OF CONTENTS

INTRODUCTION

Results of the 2009 *Summary Health Statistics for U.S. Adults National Health Interview Survey* indicate that over 29.3 million U.S. adults (12.6%) had been diagnosed with rhinosinusitis by a physician (1). In addition, the Integrated Health Interview Series for 1997-2006 noted that annual treatment expenditures totaled over $500 for 55.8% of rhinosinusitis patients (2). This is higher than the annual amount spent by patients with chronic bronchitis, hay fever, ulcer disease, and asthma. Unfortunately, healthcare expenditures for rhinosinusitis are increasing. A 2011 report by Bhattacharyya revealed that chronic rhinosinusitis (CRS) patients spent $772 more per year than non-CRS patients, and national health care costs attributed to CRS are estimated at $8.6 billion per year (3). Substantial indirect costs of rhinosinusitis also exist. Between 1997 and 2006, the number of restricted activity days due to rhinosinusitis totaled 61.2 million annually, which translates to $18.3 billion in lost opportunity cost (1, 2).

Much of this considerable annual CRS expenditure is directed toward the cost of physician office visits and pharmacotherapy. However, with over 90% sustained symptom relief, endoscopic sinus surgery (ESS) is commonly employed for medically refractory CRS (4). Over 250,000 endoscopic sinus surgeries are performed in the U.S. annually, and this number appears to be increasing (5). A report by Venkatraman and colleagues revealed that the per capita ESS rate in Medicare beneficiaries increased 19% from 1998 to 2006, despite a relatively stable rate of CRS diagnosis in the same time period (6).

Although postoperative sinonasal mucosal healing following ESS often proceeds without incident, certain patients exhibit prolonged healing, persistent mucosal edema and inflammation, and persistent paranasal sinus symptoms following sinus surgery. The underlying reasons for these prolonged healing issues are not entirely clear and have been relatively understudied. The experiments described in this thesis sought to expand knowledge of sinonasal epithelial healing on a cellular level. In a translational *in vitro* model, sinonasal epithelial wound healing properties

were examined with respect to the influence of inflammatory cytokines on wound closure time and expression of wound edge epithelial migratory and intercellular adherens junction proteins.

BACKGROUND

In the clinical arena, small studies have shown benefit in postoperative healing after ESS with the use of antibiotics, certain types of nasal dressings, and topical steroid therapy (7-10). In contrast, exposure to secondhand cigarette smoke results in poorer outcomes in children undergoing sinus surgery and poor ciliary regeneration following sinus surgery (11, 12, 13). At the cellular level, studies of sinonasal epithelial wound healing are extraordinarily limited. A study by Lazard and colleagues demonstrated that transforming growth factor (TGF)-β1 downregulated βIV-tubulin expression in a primary human nasal epithelial wounding model (14). Tan and colleagues used an *in vitro* sinonasal epithelial culture system to show that nerve growth factor accelerated epithelial wound closure rates and increased expression of E-cadherin and zonnula occludens (ZO)-1 compared to controls (15).

One important aspect potentially influencing postoperative sinonasal mucosal healing in CRS is the inflammatory microenvironment inherent to the underlying disease process. Amongst CRS inflammatory phenotypes, a T-helper (Th)1-predominant pattern of cytokines is typically seen with infectious rhinosinusitis etiologies, whereas a Th2 pattern is evident in allergic and eosinophilic sinonasal inflammation. The effect of Th1 versus Th2 skewing on postoperative sinonasal epithelial wound healing is largely unknown at this time. Numerous cytokines, cellular mediators of inflammation, and growth factors are found in CRS and nasal polyposis, representing both the Th1 and Th2 arms of the inflammatory milieu (16, 17). Common CRS inflammatory cells include eosinophils, mast cells, and neutrophils. Soluble inflammatory mediators found in CRS include histamine, numerous interleukins (ILs), interferon (IFN)-γ, granulocyte-macrophage colony stimulating factor, vascular endothelial growth factor, TGF-α1 and β1, vascular cell adhesion molecule-1, and immunoglobulin E, among others (18-27). Soluble mediators commonly associated with a Th1-predominant inflammatory profile in CRS are IFN-γ and TGF-β. Conversely, Th-2 mediators found in CRS include IL-4, IL-5, and IL-13.

Appropriate mucosal healing following sinus surgery is dependent upon timely epithelial wound closure. Certain inflammatory mediators have demonstrated profound effects on wound closure rates and wound healing properties. For example, in cultured primary human bronchial epithelium, down-regulation of E-cadherin and delayed wound closure has been demonstrated in cells treated with TGF-β1 (28). In addition, Th2-predominant IL-4 and IL-13 exposure results in decreased epithelial migration in assays of human lung Calu-3 cell wound healing, whereas exposure to Th1-predominant IFN-γ alone enhanced cell migration compared to controls (29). Epithelial healing is also delayed in a mouse model with over-expression of IL-5, a characteristic Th2 cytokine (30). Although IFN-γ alone has been shown to enhance epithelial wound closure, wounds that exhibit impaired healing and reduced collagen deposition also demonstrate elevated levels of IFN-γ and tumor necrosis factor (TNF)-α in combination in a rat model (31). Further, TNF-α is a noted inhibitor of wound healing in human and animal studies (32). For these reasons, a combination of IFN-γ and TNF-α is chosen as a positive control for impairment of wound healing in the experimental studies described herein.

Alterations in the expression, regulation, or interactions of intercellular junction and epithelial migratory proteins are noted to have a significant impact on cell migration and epithelial wound healing (33, 34). Some of the specific proteins involved in this process include annexin 2, vinculin, β1-integrin, E-cadherin, and β-catenin. Annexin 2, vinculin, and β1-integrin are heavily involved in cell migration during epithelial wound healing and are referred to as epithelial migratory proteins in the present study. E-cadherin and β-catenin are components of the epithelial cell adherens junction involved in cell-to-cell contact, and linkage to the actin cytoskeleton.

While the precise functions of annexin 2 have not been fully elucidated, this protein is known to be a calcium-dependent phospholipid binding protein involved in epithelial cellular motility, cell matrix interactions, and actin cytoskeleton linkage to membrane protein complexes (33, 35). Focal adhesions, or cell matrix adhesions, are macromolecular protein conglomerations

that provide mechanical attachment sites to the extracellular matrix and transmission of regulatory signals for cell migration that is integral to wound closure. Numerous proteins are involved in focal adhesions, including integrins and vinculin, two of the specific proteins chosen for study in these experiments. Vinculin is a membrane and cytoskeletal focal adhesion protein that associates with the actin cytoskeleton. Vinculin is important in cell migration, and its absence is associated with decreased cell spreading and focal adhesion formation, as well as inhibited extension of lamellipodia (36). Integrins play a substantial role in cell attachment to adjacent cells or to extracellular components and assist in regulation of cell migration, motility, and communication. Integrins are composed of α and β subunits, forming heterodimers, and having cytoplasmic and membrane components (37). Integrins are one of the primary proteins in focal adhesions.

Adherens junction components E-cadherin and β-catenin are transmembrane proteins which link to the actin cytoskeleton. Intact E-cadherin maintains strength of cell-to-cell contacts and reduces cell motility, whereas targeted deletions of E-cadherin domains prevents adhesion and allows cell motility (38). Somewhat similar to E-cadherin, although not as well characterized in cell motility, β-catenin activation has been shown to inhibit keratinocyte migration across wounds in studies of wound healing in skin (39). In addition, β-catenin may transmit the signal for contact inhibition which prompts cells to stop dividing upon completing a confluent epithelial layer (40).

The primary aim of the experiments described in this study was to determine if Th2 cytokines IL-4, IL-5, and IL-3 are associated with decreased sinonasal epithelial wound closure in a translational *in vitro* model. Measurements performed to satisfy this aim were via timecourse studies of wound closure percentage under conditions of individual cytokine exposure. The secondary aim of this study was to evaluate the effect of cytokine exposure on epithelial migratory and adherens junction protein expression during active sinonasal epithelial wound healing *in vitro*. Protein differences were assessed via immunofluorescence labeling/confocal

microscopy and Western immunoblot quantification. The hypothesis of this study is that exposure of sinonasal epithelial cell layers *in vitro* to characteristic Th2 inflammatory cytokines IL-4, IL-5, and IL-13 (separately) will impair wound healing rates and decrease expression of specifically-chosen epithelial migratory and intercellular adherens junction proteins compared to control sinonasal epithelial wounds not exposed to cytokines.

METHODS

Study design

The experiments described herein are designed to assess the effect of Th2 cytokine exposure on sinonasal epithelial wound healing. Exposure groups include various individual Th2 cytokines IL-4, IL-5, and IL-13 versus a positive control for inhibition of wound healing IFN-γ and TNF-α combination and media only no-cytokine exposure control. The primary outcome measure is percentage of *in vitro* epithelial wound closure assessed at repeated post-wounding time points in 4-hour increments up to 36 hours post-wounding. This experimental design is akin to a prospective cohort of wounds created at time 0, exposed to various inflammatory cytokines, and followed for 36 hours or until complete wound closure.

The secondary outcome in this study is levels of epithelial migratory and adherens junction proteins assessed during active wound healing. At a single post-wounding time point (10 hours), levels of specifically-chosen epithelial migratory and adherens junction proteins were compared amongst cytokine exposure groups. This assessment is essentially a simple comparative study in which protein levels (outcome) are compared across cytokine exposure conditions.

Controls for potential confounders, including differences in baseline protein levels, are described below in the remainder of the Methods section. Figure 1 demonstrates the proposed causal relationship of the cytokine exposure conditions, sinonasal epithelial wound healing outcomes, and wound edge protein alterations. (FIGURE 1)

Study population

Approval for this study was granted by the Emory University Institutional Review Board (protocol #00030034), and all participants gave written informed consent. Study participants were identified as persons scheduled to undergo endoscopic transnasal surgery by the principal investigator or named collaborators as part of treatment for orbital or skull base pathology (non-inflammatory controls) or as part of usual clinical care for allergic fungal rhinosinusitis (AFRS,

characteristic Th2 inflammatory CRS). Patients included in the non-inflammatory group had to be without significant clinical or radiographic evidence of inflammatory rhinosinusitis. AFRS patient inclusion criteria were based on the 1994 Bent and Kuhn diagnostic characteristics and included: atopic history, nasal polyposis, characteristic computed tomography scan findings, eosinophilic mucin on pathology, and non-invasive fungal hyphae on pathology (41). In order to be included in this study, AFRS participants were required to exhibit at least 3 of 5 diagnostic characteristics. Exclusion criteria for both groups were the presence of any of the following: cystic fibrosis, immune deficiency, autoimmune conditions, granulomatous disorders, aspirin-exacerbated respiratory conditions or use of steroid medications within 7 days prior to surgery. Vulnerable populations such as prisoners, institutionalized individuals, and pregnant women were also excluded.

Primary sinonasal epithelial air-liquid interface cell culture

During endoscopic transnasal surgery, sinonasal tissue was biopsied from paranasal sinus mucosal lining using standard endoscopic transnasal instrumentation. Biopsied sinonasal tissue was placed into RPMI 1640 media (Invitrogen, Carlsbad, CA). Antibiotic/antimycotic (Invitrogen, Carlsbad, CA) at 2X final concentration was added to the RPMI 1640 media to maintain sterility, and sinonasal tissue was digested with protease isolated from *Streptococcus griseus* (Sigma-Aldrich, St. Louis, MO) for 90-120 minutes at 37°C or overnight at 4°C. The protease reaction was stopped with heat inactivated fetal bovine serum. Tissue pieces were mechanically separated from the supernatant and discarded. The supernatant was centrifuged for 5 minutes (950 rpm, room temperature). The cell pellet was resuspended in Bronchial Epithelial Growth Medium (BEGM), consisting of Bronchial Epithelial Basal Medium (BEBM) supplemented with EBM SingleQuot additives (Lonza, Walkersville, MD), antibiotic/antimycotic (Invitrogen, Carlsbad, CA), and nystatin (Sigma-Aldrich, St. Louis, MO). Epithelial cells were isolated from fibroblasts by incubating at 37°C for 2 hours in a collagen-coated P100 tissue

culture-treated petri dish. Following incubation, epithelial cell-rich supernatant was placed into collagen-coated T75 cell culture flasks (Corning, Corning, NY). Primary sinonasal epithelial cell cultures were maintained at 37°C, 5% CO_2, 95% humidity, and BEGM media was changed every 48-72 hours.

Once the cell layers reached 85% confluence in T75 culture flasks, cells were split to Transwell inserts for eventual growth at the air-liquid interface. Initially, cells were washed with Ca^{2+} and Mg^{2+} free Hanks Balanced Salt Solution (HBSS-) (Sigma-Aldrich, St. Louis, MO) and trypsinized with Trypsin-EDTA (Invitrogen, Carlsbad, CA). After appropriate cell release, soybean trypsin inhibitor was added to stop the trypsin reaction. Cells were then centrifuged for 5 minutes at 950 rpm and resuspended in BEGM. Cells were seeded onto collagen-coated Transwell inserts of 6.5 or 24 mm diameter and 0.4 μm pore size (Corning, Corning, NY).

Cells were maintained on Transwell inserts with BEGM on the apical and basal surfaces until confluence was confirmed by light microscopy. Media was changed every 48-72 hours. At confluence on Transwell inserts, apical media was removed and basal media was changed to air-liquid interface (ALI) media. The base of ALI media was a 50:50 mixture of BEBM (Lonza, Walkersville, MD) and DMEM high glucose (Invitrogen, Carlsbad, CA). ALI media was supplemented with BEBM SingleQuots, antibiotic/antimycotic, 10 mM retinol (Sigma-Aldrich, St. Louis, MO), and bovine serum albumin (Sigma-Aldrich, St. Louis, MO). Over the subsequent 2-6 weeks, cell layers polarized and differentiated at the air-liquid interface. Polarization and differentiation was confirmed by identification of beating cilia under phase-contrast light microscopy. Before use in wounding experiments, cells were allowed to stabilize for at least 6-10 additional days. These primary sinonasal epithelial culture methods are based upon the methods of Lane and colleagues (42). (FIGURE 2)

In vitro sinonasal epithelial wounding experiments

Confluent, mature, polarized, differentiated, ciliated primary sinonasal epithelial cell cultures from non-inflammatory patients were used for *in vitro* wounding experiments. Non-inflammatory sinonasal epithelial cultures were used in order to reduce any undue influence in wound closure rates and/or migratory and junctional protein changes that would potentially occur from inherent epithelial properties of source inflammatory CRS patients. This also allows isolation of the effects of cytokine exposure in the laboratory setting.

The non-inflammatory sinonasal epithelial cultures were initially exposed to specifically-chosen cytokines for 24 hours prior to wounding. Cytokines are added to ALI media in the basal Transwell culture chamber at the following final concentrations: recombinant human Th2 cytokine IL-4 (50 ng/ml, R&D Systems, Minneapolis, MN) (29, 43), recombinant human Th2 cytokine IL-5 (200 ng/ml, R&D Systems) (44), recombinant human Th2 cytokine IL-13 (50 ng/ml, R&D Systems) (29), wound closure inhibitor positive control IFN-γ (100 units/ml, Genentech, San Francisco, CA) (45) and recombinant human TNF-α (500 ng/ml, BioVision, Mountain View, CA) (46) combination. Chosen concentrations are moderate to high concentrations based upon available literature and previous experience, in order to appropriately stimulate an effect, as available tissue and resources did not allow for extensive dose finding studies.

After 24 hour cytokine exposure, sterile linear mechanical wounds were created in the sinonasal epithelial cell layers. A total of 12 wounds per cytokine exposure group were performed for analysis in this timed wound closure experiment. Every 4 hours for 36 hours, microscopic photographs of each wound were taken with a Zeiss Axiovert 35 microscope with MRc5 AxioCam (Zeiss Microimaging, Thornwood, NY), providing images at 9 post-wound time points. Using ImageJ image analysis software (National Institutes of Health, Bethesda, MD) wound edges were outlined, and wound area was recorded for each picture. Wounds were followed until the 36-hour post-wounding time point or until complete wound closure. (FIGURE 3) Throughout

the wounding experiments, cells were maintained at 37°C, 5% CO_2, 95% humidity unless microscopic photographs were actively being taken.

Over the 36 hour timecourse, a maximum of 10 wound areas could be recorded for each individual wound – initial wound area and 9 post-wound areas. The percentage wound closure was then calculated for each post-wound time point. Repeated measures analysis of variance (ANOVA) with one between-group variable and one within-group variable was used to assess differences in wound closure over time (within-group, repeated measure), cytokine group differences (between-group), and any interactions between these measures. Statistical significance for the overall ANOVA was set a $p<0.05$. Although group sizes of 12 wounds per group are somewhat small and it is difficult to ensure a normal distribution in wound closure percentage values amongst the population from which these samples are drawn, a repeated measures ANOVA was chosen for statistical analysis after consideration of various alternatives. First, an assessment of normal data distribution (skewness statistic divided by standard error of skewness statistic) was performed for each cytokine exposure group at each post-wounding time point in order to provide some estimation of whether each sample set was normally distributed, and most of the individual sample sets were normally distributed. Second, there is no non-parametric equivalent that would be appropriate for an analysis of this kind. Although a combination Kuskall-Wallis and Friedman nonparametric testing would be able to assess for individual main effects of wound closure percentage over time and cytokine group differences, these tests are not able to evaluate time-group interaction as the repeated measures ANOVA can. The importance of identifying time-group interactions is integral to appropriately assessing the outcome of individual cytokine effects on sinonasal epithelial wound closure in this study.

Migratory and adherens junction protein assessments during wound closure

Based upon the sinonasal epithelial wound timecourse experiments described above, a panel of specifically-chosen migratory and adherens junction proteins was analyzed for individual

cytokine group differences in subsequent *in vitro* wounding experiments. Timecourse wounding experiments identified the 8-12 hour post-wounding timeframe as the time at which the greatest discrepancy in wound closure rates existed amongst individual cytokine exposure groups. Further, Th2 cytokine IL-4 had the largest percentage of unhealed wounds at the 36-hour experiment end and graphically exhibited slower wound closure rates than IL-5 or IL-13. (These findings are described further in the Results section.) Therefore, the Th2 cytokine chosen for further investigation of active wound healing protein alterations was IL-4.

Experiments for wound edge protein alterations were performed by, once again, incubating primary, mature, polarized, differentiated, ciliated sinonasal epithelial cells from non-inflammatory tissue with IL-4 (50 ng/ml), IFN-γ (100 units/ml) and TNF-α (500 ng/ml) combination, or no-cytokine control for 24 hours at 37°C, 5% CO_2, 95% humidity. After 24 hour cytokine pre-incubation, sterile linear mechanical wounds were created in the sinonasal epithelial cell layers. At approximately the 10-hour post-wounding time point, wound closure experiments were stopped and proteins were assessed quantitatively via image analysis of immunofluorescent labeling and confocal microscopy, as well as semi-quantitatively via Western immunoblotting.

Antibodies and reagents

A panel of epithelial migratory and adherens junction proteins was analyzed with the following antibodies: anti-annexin 2 (Abcam, Cambridge, MA), anti-β1-integrin (Novus Biologicals, Littleton, CO), anti-vinculin (Novus Biologicals, Littleton, CO), anti-E-cadherin (Sigma-Aldrich, St. Louis, MO), and anti-β-catenin (Invitrogen, Carlsbad, CA). Alexa-488 and Alexa-546-conjugated secondary antibodies (Invitrogen, Carlsbad, CA) were used for immunofluorescent staining. Horseradish peroxidase-conjugated secondary antibodies (Jackson Immunoresearch Laboratories, West Grove, PA) were used for Western immunoblotting. All remaining immunofluorescent staining and Western immunoblot reagents were obtained from Sigma-Aldrich, unless stated otherwise.

Immunofluorescent labeling and confocal microscopy for in vitro wounding experiments

Sinonasal epithelial wound edge migratory and adherens junction protein expression and localization were examined by immunofluorescence labeling and confocal laser microscopy. Epithelial cell samples were fixed and permeabilized in methanol for 20 minutes at -20°C (annexin 2, β1-integrin, E-cadherin, β-catenin) or paraformaldehyde for 30 minutes at room temperature followed by 10% Triton X-100 for 30 minutes at room temperature (vinculin). The remaining immunofluorescence staining steps were performed at room temperature. Following fixation, samples were washed with HBSS with Mg^{2+} and Ca^{2+} (HBSS+). Non-specific staining was blocked with 3% bovine serum albumin in HBSS+ for 1 hour. Primary antibodies were diluted in blocking buffer at the following concentrations: annexin 2 (1:50), β1-integrin (1:100), vinculin (1:300), E-cadherin (1:100), and β-catenin (1:100). These concentrations are based on antibody manufacturer recommendations or prior use in our laboratories. Samples were incubated with primary antibodies for 1 hour. Following incubation with primary antibodies, samples were washed in HBSS+ and incubated with Alexa Fluor secondary antibodies (1:500 in blocking buffer) for 1 hour. Samples were washed a final time in HBSS+, mounted on slides with p-phenylenediamine anti-quench reagent, and sealed.

Stained cell layers were examined using a Zeiss LSM510 laser scanning confocal microscope coupled to a Zeiss 100M Axiovert with a 40× Pan-Apochromat oil lens. Fluorescent dyes were imaged sequentially to eliminate cross talk between channels, and images were processed with Zeiss LSM5 image browser software.

In order to provide quantitative assessments of specific protein changes at epithelial wound edges by cytokine exposure group during active wound healing, a single representative wounding experiment, stopped during active wound healing at approximately 10 hours post-wounding, was performed as described above. Eight to ten confocal microscopy wound edge

photographs were taken for each specified protein per cytokine exposure condition. The wound edge photographs were taken from multiple wounds for each cytokine exposure condition in order to provide a representative sample of wound edges. However, in order to reduce staining and confocal microscopy variability as much as possible, all aspects of the experiment were performed on the same day across cytokine exposure groups: epithelial wounding, immunofluorescent staining, and confocal imaging. Further, confocal microscopy settings were standardized to a single control wound edge image and the same settings were used across all cytokine exposure conditions for each protein studied.

Quantitative pixel intensity analysis was performed with the ImageJ image analysis software. The wound edge epithelial area was outlined on the ImageJ program. Pixel density was recorded for the outlined area, and the pixel density was divided by the area. Pixel density per area differences were compared amongst cytokine exposure groups for each specified protein. (FIGURE 4) Statistical analysis was performed with non-parametric Kruskall-Wallis testing across all cytokine exposure groups with post-hoc Mann Whitney U testing to determine individual group differences. Non-parametric testing was performed due to small sample size and the inability to ensure that the population from which the sample was drawn was normally distributed. Differences were considered statistically significant when the p-value was <0.05.

Cell lysis and Western immunoblotting for in vitro wounding experiments

To further assess epithelial migratory and adherens junction protein differences during active wound closure amongst cytokine exposure groups, Western immunoblotting was performed for protein semi-quantitation. At the 10-hour post-wounding time point, cells were washed with HBSS+ and scraped into RIPA buffer (20 mM Tris, 150 mM NaCl, 2 mM EDTA, 2 mM EGTA, 1% Na deoxycholate, 1% Triton X-100, 0.1% SDS, pH 7.4) with a protease inhibitor cocktail (Sigma-Aldrich, St. Louis, MO). Complete cell lysis was ensured by sonicating samples on ice and rotating for 30 minutes at 4°C. Nuclear debris was removed from samples by

centrifugation (1,000 x g, 5 minutes), and sample protein concentrations were normalized by bicinchoninic acid assay (Thermo Fisher Scientific, Waltham, MA). Lysates were boiled in SDS sample buffer containing 10% 2-mercaptoethanol for 10 minutes. Protein samples were run on SDS-polyacrylamide gels and transferred to nitrocellulose membranes for Western immunoblotting.

Primary antibodies for Western immunoblots were used at the following concentrations: annexin 2 (1:500), β1-integrin (1:2000), vinculin (1:400), E-cadherin (1:200), and β-catenin (1:300). These concentrations are based on antibody manufacturer recommendations or prior use in our laboratories. Protein loading control for these experiments was glyceraldehyde 3-phosphate dehydrogenase (GAPDH), which demonstrates little fluctuation with active epithelial cell migration. Finally, to ensure protein fluctuations were seen as the result of epithelial cell migration and wound healing rather than cell death, apoptosis marker poly-ADP ribose polymerase (PARP) levels were also assessed by Western immunoblot.

Semi-quantification of Western immunoblot protein levels was performed for each experimental run by using image analysis to normalize protein density for each specified epithelial migratory or adherens junction protein to the GAPDH protein loading control for that experiment. Normalized protein levels were collated across 2-4 experimental runs for each specified protein in order to provide representative distributions of protein density. These experiments were performed in order to assess protein levels by a method complimentary to immunofluorescence labeling. No statistical analysis was performed for Western blot experiments due to small sample sizes.

Sinonasal tissue biopsy for frozen section

One consideration of a potential confounding factor in the analysis of sinonasal epithelial wound healing experiments is the possibility that baseline protein differences may occur amongst cytokine-exposed and non-cytokine-exposed tissues. If baseline differences were present, protein

alterations identified during active wound healing would be less reliable and more difficult to interpret. For this reason, it was determined that baseline protein differences in the same panel of epithelial migratory and adherens junction proteins would be assessed from human sinonasal tissue biopsies taken at the time of transnasal endoscopic sinus surgery. As stated above, non-inflammatory participants were undergoing sinus surgery as an approach to orbital or skull base pathology, and AFRS participants represent a group of CRS patients with a characteristic Th2 inflammatory profile and defined diagnostic criteria. Tissue biopsies from surgical patients are used in this portion of the experiment for two reasons. First, the use of tissue specimens directly from surgical patients provides a translational corollary to substantiate the *in vitro* wounding experiments. Second, due to the length of time necessary to grow primary sinonasal epithelial cells in culture and the inherent limitations of primary cell culture, culture samples were not available for extensive baseline epithelial migratory and adherens junction protein assessments following initial 24 hour cytokine exposure, and *in vivo* tissue biopsies are therefore used as a surrogate measure.

Sinonasal tissue was biopsied from paranasal sinus lining (non-inflammatory control) or obvious polyposis (AFRS) during endoscopic transnasal surgery using standard endoscopic transnasal instrumentation. Biopsied tissue was placed into TissueTek® O.C.T. compound (Sakura Finetek USA, Torrence, CA), snap frozen on dry ice, and stored at -80°C for frozen tissue sectioning. Alternatively, for protein quantification, biopsied tissue was snap frozen in cryovials and stored at -80°C until further use. Frozen tissue sections (8µm thickness) were cut on a Leica CM1510 cryostat (Leica Microsystems, Bannockburn, IL) and placed on positively charged slides.

Immunofluorescent labeling and confocal microscopy on frozen sinonasal tissue sections

Immunofluorescent staining was performed as described above for epithelial wounding experiments. The sole exception to the above protocol is that blocking buffer for tissue staining was 5% normal goat serum in HBSS+.

Similar to the quantitative assessment of protein changes in wound healing experiments, quantitative evaluation of baseline protein levels in sinonasal tissue sections were performed. Images from seven to nine independent non-inflammatory control and nine to ten independent AFRS participant samples were captured by confocal microscopy photography for each specified protein. In order to control staining and confocal microscopy variability, immunofluorescent staining and confocal imaging was performed on the same day for each specified protein. Confocal microscopy settings were also standardized to a single tissue image and the same settings were used across all non-inflammatory and AFRS participant specimens for each protein studied.

Quantitative pixel intensity analysis was performed with the Image analysis software. The sinonasal tissue epithelial area was outlined on the ImageJ program. (FIGURE 5) Pixel density was recorded for the outlined area, and the pixel density was divided by the area. Pixel density per area differences were compared between non-inflammatory control and Th2-predominant AFRS groups for each specified protein. Statistical analysis was performed with non-parametric Mann Whitney U test due to small sample size per group and the inability to ensure that the population from which the sample was drawn was normally distributed. Differences were considered statistically significant when the p-value was <0.05. Of note, as the *in vivo* human sinonasal tissue biopsies are taken at rest, rather than during active epithelial migration or wound healing, it is expected that epithelial migratory protein levels should not differ between control and AFRS groups at baseline.

Cell lysis and Western immunoblotting on sinonasal tissue biopsies

Baseline epithelial migratory and adherens junction protein differences were further evaluated on available frozen sinonasal tissue sections by semi-quantitation with Western immunoblotting. Previously frozen tissue specimens were thawed and homogenized in RIPA buffer. The remainder of steps for Western immunoblotting procedures is as described above for *in vitro* wounding experiments.

Again, semi-quantification of Western immunoblot protein levels was performed with image analysis to normalize protein density for each protein of interest to the GAPDH protein loading control. Normalized protein levels were collated across 3 total experimental runs for each specified protein in order to provide representative means and standard deviations. These experiments were performed in order to assess protein levels by a method complimentary to immunofluorescence labeling. No statistical analysis is performed for tissue biopsy Western blot experiments.

RESULTS

In vitro sinonasal epithelial wound healing studies with cytokine exposure

Timecourse wound closure studies under cytokine exposure conditions were analyzed by repeated measures ANOVA with one between-group variable (cytokine exposure) and one within-group variable (time, repeated measure). Mean percent wound closure for each cytokine exposure group at each post-wounding time point is presented in TABLE 1. A measure of normal distribution (skewness statistic divided by standard error of the skewness statistic) was also performed for each group. Of note, with few exceptions, the vast majority of sample value sets are normally distributed (value < 2) until the 32 and 36 hour post-wounding time points. It is not surprising that these later post-wounding time points have skewed distributions, as many of the wounds had achieved 100% closure by these time points.

As expected, there was a significant main effect of time ($p<0.001$), with all cytokine exposure groups exhibiting increasing mean wound closure percentage over time. There was also a significant main effect of cytokine exposure group in the overall repeated measures ANOVA ($p<0.001$). Tukey post-hoc analysis indicates that, as hypothesized, the no-cytokine control condition was significantly different from the wound closure inhibition positive control IFNγ-TNFα condition ($p=0.005$) and from the IL-4 condition ($p=0.001$). However, unexpectedly, the IL-5 exposure condition followed the no-cytokine exposure condition closely and did not exhibit significant impairment in wound closure. The IFNγ-TNFα condition was significantly different from the IL-5 condition ($p=0.023$), as was the IL-4 condition ($p=0.005$). Also unexpectedly, the IL-13 condition was not significantly different from any of the other exposure conditions, including positive or negative controls, IL-4, or IL-5. (FIGURE 6)

Although there are significant individual main effects of time and cytokine exposure group in the timed sinonasal epithelial wound closure analysis, as described above, the most crucial finding in the repeated measures ANOVA is the significant time by cytokine exposure interaction ($p<0.001$). Tukey post-hoc analysis of this interaction reveals that multiple individual

significant differences exist across all post-wounding time points from 8 to 36 hours. (TABLE 2) There were no significant cytokine group differences at the 4 hour post-wounding time point. Indicating relatively good experimental conditions, the positive control IFNγ-TNFα (poor wound closure) condition was significantly different from the no-cytokine control at all post-wounding time points from 8 to 28 hours. However, somewhat surprisingly, the IFNγ-TNFα wounds had increased wound closure rate in the 32-26 hour period and did not differ from the no-cytokine control at these time points. Th2 cytokine exposure condition IL-4 differed from no-cytokine control at all post-wounding time points after 4 hours and did not have accelerated wound closure in the 32-36 hour time period as the IFNγ-TNFα wounds did. Interestingly, the IL-5 and IL-13 exposure conditions seemed to mirror the no-cytokine control and exhibited multiple significant differences versus the IFNγ-TNFα and IL-4 exposure conditions across numerous post-wounding time points from 8 to 36 hours.

At the completion of the cytokine exposure wound closure timecourse experiment, 9 of 12 (75%) no-cytokine exposure control wounds were completely closed. Likewise, 10 of 12 (83.3%) IL-5 exposed wounds and 9 of 12 (75%) IL-13 exposed wounds were completely closed. However, only 6 of 12 (50%) IFNγ-TNFα exposed wounds and 3 of 12 (25%) IL-4 exposed wounds were completely closed at the 36-hour end of the timecourse experiment. Mean percentage wound closure at the completion of the 36-hour timecourse was 98.41% ± 3.43% for the no-cytokine exposure control wounds, 99.38% ± 2.14% for IL-5 exposed wounds, 95.83% ± 7.58% for IL-13 exposed wounds, 96.50% ± 5.99% for IFNγ-TNFα exposed wounds, and 85.02% ± 18.46% for IL-4 exposed wounds. Taken together, these results indicate that exposure to IL-4 during sinonasal epithelial wound healing *in vitro* significantly delays wound healing.

Epithelial migratory and adherens junction protein assessment during active sinonasal epithelial wound healing under cytokine exposure conditions

Based upon the sinonasal epithelial wound healing timecourse experiment results above, additional investigation of potential mechanisms for impaired wound healing in the IL-4 cytokine exposure group was performed. The graphical representation of wound closure percentage indicates that the most disparate rates of wound closure between no-cytokine control and the IL-4 exposure group occurred between 8 and 12 hours post-wounding. (FIGURE 7) Therefore, the *in vitro* cytokine exposure sinonasal epithelial wound healing experiments were repeated as previously described. However, to investigate epithelial migratory and adherens junction protein differences by cytokine exposure group, the experiments were stopped at the 10 hour post-wounding time point and investigated for protein differences via immunofluorescence staining/confocal microscopy and Western immunoblots.

Pixel intensity analysis of sinonasal epithelial wound edges, as assessed by immunofluorescence staining/confocal microscopy revealed significant differences in protein levels for all proteins evaluated, except β1-integrin. By Kruskall-Wallis nonparametric analysis, significant protein differences were identified across cytokine exposure conditions for annexin 2, vinculin, E-cadherin, and β-catenin. (TABLE 3) Post-hoc analysis by nonparametric Mann Whitney U testing identified significant individual cytokine exposure group differences, as exhibited in Figure 8. (FIGURE 8) Notable findings include significantly decreased wound edge levels of annexin 2 ($p=0.001$), vinculin ($p=0.002$), and β-catenin ($p=0.034$) with IL-4 exposure versus no-cytokine control. Wound edge levels of vinculin ($p=0.004$) and E-cadherin ($p=0.001$) were also decreased in the positive control IFNγ-TNFα exposure condition versus no-cytokine exposure control. Consistent with previously referenced keratinocyte experiments by Stojadinovic and colleagues (39), β-catenin pixel intensity analysis results revealed an increase in wound edge pixel density in the IFNγ-TNFα exposed condition versus IL-4 exposed wounds (0.006) and no-exposure control ($p = NS$) – as anticipated with decreased cell migration and wound closure.

To further assess epithelial migratory and adherens junction protein levels and compliment pixel intensity analysis at the 10 hour post-wounding time point, Western

immunoblot analysis of protein levels was also performed. Figure 9 demonstrates example Western immunoblot results for each of the 5 specifically chosen proteins in the above panel. (FIGURE 9) Further, in each run of Western immunoblot experiments, the density of protein of interest was normalized to GAPDH protein loading control. Graphical representation of these normalized protein levels across multiple Western immunoblot runs is also shown, in order to better demonstrate median protein level changes across experimental trials. Of note, apoptosis marker PARP cleaved product levels were also assessed in Western immunoblot analysis of wound closure experiments. No differences in PARP cleavage product levels were seen across cytokine exposure conditions, indicating that differences in epithelial migratory and adherens junction proteins are not likely to be due to differences in cell death across cytokine exposure groups.

Visual inspection of the graphical patterns for each protein reveals consistent results for annexin 2 across immunofluorescence (FIGURE 8) and Western immunoblot (FIGURE 9) experiments, with decreased protein levels in IL-4 and IFNγ-TNFα exposure conditions versus no-cytokine exposure control. Graphical results for β1-integrin are variable across immunofluorescence and Western immunoblot experiments, although notably no significant results were seen in the immunofluorescence experiment and only 2 trials were performed for Western immunoblots. No conclusions are drawn based upon β1-integrin protein changes from these experimental comparisons. Graphical representation of protein patterns are also consistent for β-catenin across cytokine exposure conditions in the immunofluorescence and Western immunoblot experiments, with IFNγ-TNFα exposure demonstrating increased protein levels and IL-4 exposure demonstrating decreased protein levels versus no-cytokine control. Finally, vinculin and E-cadherin experiments reveal consistent decreases in protein levels with IL-4 exposure in both immunofluorescence and Western immunoblot experiments. However, in contrast to immunofluorescence experiments, vinculin and E-cadherin protein levels are decreased in immunofluorescence experiments and increased in Western immunoblot

experiments with IFNγ-TNFα exposure (compared to no-cytokine control). Due to the small number of experimental trial for Western immunoblots, no statistical analysis is performed. The results and comparisons described above are simply drawn from visual inspection of graphical patterns in Figures 8 and 9.

These results indicate that certain epithelial migratory and adherens junction proteins (annexin 2, vinculin, E-cadherin, and β-catenin) show consistent decreases in protein levels during active wound healing under IL-4 exposure with 2 different methods of protein assessment – immunofluorescence labeling/confocal microscopy and Western immunoblots. Some skepticism in interpretation of the vinculin and E-cadherin results is appreciated, as the positive control IFNγ-TNFα exposure condition resulted in increased protein levels in the Western immunoblot experiments versus decreased protein levels in the immunofluorescence experiments. Substantial additional investigations would be necessary to better delineate the true changes in vinculin and E-cadherin with IFNγ-TNFα exposure. β1-integrin results are inconsistent and no conclusions are able to be drawn from these experiments regarding changes in β1-integrin levels with *in vitro* sinonasal epithelial wound healing.

Epithelial migratory and adherens junction protein assessment at baseline from sinonasal tissue biopsies

One concern, and potential confounder, resulting from the timecourse wounding experiments described above is the possibility of inherent baseline epithelial migratory and adherens junction protein differences. As described in the Methods section, in order to condition the sinonasal epithelial cells prior to wounding, cytokines are added to the basal media compartment of the Transwell system 24 hours prior to cell layer wounding. During this 24 hour period, it is possible that baseline protein changes may occur under the influence of cytokines. Therefore, baseline protein levels were assessed in the sinonasal epithelial sections.

Although the most ideal and controlled method to assess for baseline epithelial migratory and adherens junction protein changes in this experiment would be to evaluate *in vitro* cell layers for protein levels following cytokine exposure and prior to wounding. However, due to the limited number of available primary sinonasal epithelial cell cultures and the length of time required for the cultures to grow and mature to differentiation (approximately 8 weeks), a surrogate baseline measure was chosen. Surgical biopsies were taken from patients undergoing endoscopic transnasal surgery, sectioned by frozen sectioning techniques, and stained by immunofluorescence for the same panel of proteins in the *in vitro* wounding experiments above. Biopsies from the paranasal sinus mucosa of non-inflammatory patients represented the control condition, and biopsies from nasal polyps and paranasal sinus mucosa of AFRS patients (a characteristic Th2 inflammatory rhinosinusitis disease) represented the Th2 inflammatory condition. Pixel density per epithelial area from confocal microscopy images (representing epithelial protein content) was assessed in sinonasal biopsies from at least 7 non-inflammatory patients and 9 AFRS patients for each protein. In addition to serving as a surrogate marker for baseline epithelial migratory and adherens junction protein levels, the evaluation of protein levels in sinonasal biopsies also adds and *in vivo* translational aspect to this experimental design and draws a parallel to the assessment of baseline protein levels that would truly be observed in the *in vivo* state.

Immunofluorescence staining and confocal microscopy pixel intensity analysis of sinonasal epithelial sections did not reveal any significant differences in protein levels between control and Th2-predominant AFRS, as assessed by non-parametric Mann Whitney U testing. (TABLE 4 and FIGURE 10) It should be noted that aside from any statistical comparison, median pixel intensity comparisons between control and AFRS groups are visibly relatively equivalent across all proteins evaluated. Further, across the 5 proteins studied, there was quite a bit of data variability in the pixel intensity for both the control and AFRS groups. These imaging and data characteristics support the lack of statistical significance seen in these analyses. (FIGURE 11)

Available frozen epithelial tissue sections were also used to isolate total protein and confirm certain baseline sinonasal migratory protein levels. For annexin 2 and vinculin, at least 3 Western immunoblot trials were performed. For each experimental trial, Western immunoblot protein density from each patient sample was normalized to GAPDH loading control. Normalized protein density was combined across the experimental trials for each protein and results are presented in Figure 12. (FIGURE 12) Visual analysis reveals no discernable pattern or difference between non-inflammatory control samples (C) and AFRS samples (A). These results support baseline sinonasal tissue biopsy immunofluorescence pixel density analysis presented discussed above. Due to available protein isolated from tissue samples and experimental variability, 3 Western blot trials could not be performed for β1-integrin, E-cadherin, and β-catenin. Therefore, Western blot data is not presented for these proteins.

The results seen in sinonasal tissue biopsies from non-inflammatory control and Th2-predominant AFRS patients support the notion that epithelial migratory and adherens junction proteins do not appear to be significantly different at baseline. Therefore, inherent baseline protein differences are unlikely to be a confounding factor in this data analysis and correction or stratification for any baseline protein differences is unnecessary.

DISCUSSION

Although prior studies of wound healing in sinonasal epithelium have been limited, it has been demonstrated that certain soluble mediators have specific effects in augmenting or inhibiting wound closure (14, 15). Based upon the importance of Th2 cytokines IL-4, IL-5, and IL-13 in certain, largely allergic, types of inflammatory CRS, the experiments in this study were undertaken to determine the effects of these individual cytokines on sinonasal epithelial wound healing *in vitro*. The results of these translational studies are anticipated to lead to future clinical understanding of the mechanisms behind poor or delayed healing following paranasal sinus surgery.

Our experimental results demonstrated reduced sinonasal epithelial wound closure with exposure to Th2 cytokine IL-4, as hypothesized. At the completion of the timecourse wound closure studies, only 25% of IL-4 exposed wounds were completely closed, and the overall mean wound closure percentage for IL-4 exposed wounds was 85.02% ± 18.46%. Further, percentage closure of IL-4 exposed wounds differed from the no-cytokine exposure condition at every post-wounding time point from 8 to 36 hours. These results indicate a substantial inhibitory effect of IL-4 exposure on sinonasal epithelial wound healing.

In contrast to the deleterious effect of IL-4 exposure on sinonasal epithelial wound healing, IL-5 and IL-13 exposure conditions did not differ significantly from the no-cytokine exposure condition at any of the post-wounding time points. Possible reasons for these findings include, first, the lack of a true effect on sinonasal epithelial wound healing caused by IL-5 or IL-13. Although this is a small study, the wound closure percentage measurements appear fairly precise, without extensive variability across time points. However, as only a single cytokine concentration was tested, the potential that this chosen concentration was not appropriate to inhibit sinonasal epithelial wound healing should be considered. Prior studies of Th2 cytokine effects on sinonasal epithelial wound healing are not available for comparison. Although IL-5 and IL-13 exposure conditions have led to impaired wound healing in mouse models and lung cells *in*

vitro, these results may not translate to sinonasal epithelial wound healing due to organ system and species differences (29, 30). Future studies will better elucidate the precise role of IL-5 and IL-13 on sinonasal epithelial wound healing and either support or refute the findings in the current experiments.

With regard to observed protein alterations at the wound edge in this study, epithelial migratory and focal adhesion proteins annexin 2 and vinculin were reduced in actively healing IL-4 exposed wounds as identified by both immunofluorescence labeling pixel intensity analysis and Western immunoblot quantification. These reduced epithelial migratory protein levels coincide with the decreased wound closure percentage seen under IL-4 exposure conditions. Whether IL-4 exposure has a direct effect on reduction of annexin 2 or vinculin as the mechanism for impaired epithelial wound closure has not been fully evaluated in this study. However, this is a possibility and provides interesting hypotheses for future investigations.

The effects of IL-4 and IFNγ-TNFα exposure on wound edge β-catenin levels in this study are interesting. β-catenin is an adherens junction protein involved in strengthening cell-to-cell contact. In keratinocytes, increases in β-catenin lead to increases in cell-cell contact and correspondingly to decreased cell migration (39). In our study, a significant increase in β-catenin was seen at the wound edge in IFNγ-TNFα exposed cells, in conjunction with decreased wound closure – similar to the pattern seen in keratinocytes. In contrast, IL-4 exposed sinonasal epithelial wounds exhibited decreased β-catenin staining at the wound edges, as well as decreased cell migration. Potential mechanisms for this decrease in β-catenin and decreased wound closure under IL-4 influence are not fully elucidated at this time. It is possible that the reduced β-catenin seen in this situation results from mechanisms unrelated to wound closure or cell migration activities. An extensive literature search yields little evidence to explain these findings, other than a 2001 study of gene expression from activated Th1 cells which revealed high expression of β-catenin, as opposed to activated Th2 cells which did not exhibit increased β-catenin expression

(47). Additional experiments will be necessary to fully understand the wound edge β-catenin patterns evidenced in sinonasal epithelial wound healing.

No distinct conclusions may be drawn regarding sinonasal epithelial wound edge alterations in E-cadherin, as the experimental results in this study were rather variable. Compared to wounds without cytokine exposure, IL-4 exposed wounds demonstrated a decreased E-cadherin expression pattern by immunofluorescence and Western immunoblot; however, these results were not statistically significant and will require additional investigation to better understand the true pattern of change. Moreover, the pattern of E-cadherin change in wounding experiments that was seen in the positive control IFNγ-TNFα exposed condition was variable between immunofluorescence (decreased expression) and Western immunoblot (increased expression). This makes drawing conclusions about E-cadherin expression across these sinonasal epithelial wounding studies very difficult, and additional investigations will be necessary to determine the role of E-cadherin in sinonasal epithelial wound healing and cell migration.

This study has resulted in interesting data regarding sinonasal epithelial wound healing in a translational model. Based upon these findings, the Th2 cytokine which inhibits sinonasal epithelial wound healing to the greatest degree is IL-4, whereas IL-5 and IL-13 appear to have no significant effect on wound healing in sinonasal epithelium. Reduced cell migration in sinonasal epithelium during wound healing under the influence of IL-4 is likely related to decreased expression of migratory proteins annexin 2 and vinculin. However, the precise mechanisms of these protein changes in relation to IL-4 exposure remain to be determined.

Experimental limitations

Certain limitations must be considered for this study, as with any scientific experiment or clinical trial. The first limitation of the experiments described herein is the use of a single cytokine concentration for each of the cytokine exposure conditions during sinonasal epithelial wound healing studies. Although the cytokine concentrations in these experiments were chosen

based upon literature references or prior laboratory experience, it is possible that varying the cytokine concentrations would have produced different effects in wound closure percentage across groups. In addition, increasing or decreasing the cytokine concentrations could potentially result in different expression of epithelial migratory and/or adherens junction protein levels. An ideal experiment would be to perform epithelial wound healing and protein expression studies while titrating increasing concentrations of each individual cytokine. However, due to sinonasal tissue and resource limitations, as well as the 2 month time period required for mature primary sinonasal epithelial air-liquid interface cell cultures, it was not possible to perform these studies with numerous concentrations of each cytokine condition. Similar to the potential drawback of using a single cytokine concentration, it may be argued that limiting experimental exposure to a single cytokine in sinonasal epithelial wound healing studies would also be a downfall. In the living human, there are innumerable cellular and soluble mediators that interact amongst each other and with surrounding cells. However, while the experimental conditions in this study do not precisely mimic the *in vivo* cytokine exposure during wound healing, separating the cytokine exposures to a single mediator allows controlled determination of the effects of one cytokine mediator, which is important for early and preliminary experiments. Once these individual effects are known, experiments may be expanded to assess cytokine interactions and their effects on sinonasal epithelial wound healing.

The second limitation of this study is the use of immunofluorescence labeling and confocal microscopy image pixel intensity analysis for quantification of sinonasal tissue protein levels. Although this technique has been previously used in similar studies, there is inherent variability in immunofluorescence staining and confocal microscopy image acquisition (48, 49). In order to control this variability as much as possible, immunofluorescence labeling sessions for each protein studied were performed on the same day and confocal images for each protein were acquired on the same day. Further, within each protein, confocal microscopy image acquisition settings were set to a single control sinonasal tissue specimen and retained throughout all images

obtained for that protein set. Finally, a single investigator performed all image analysis pixel density measures. Another issue to consider with respect to the use of immunofluorescence pixel intensity analysis for quantification of protein levels is the potential for bias in selection of epithelial sections for imaging. It is possible that available epithelium and wound edges within a particular tissue section may be extensive, allowing the investigator to select the most promising areas to photograph for pixel intensity analysis. However, in reality, due to the nature of tissue processing and freezing artifacts occurring in the majority of tissue and cell culture sections, a minimal number of appropriate images were identified per slide. Epithelial regions selected for imaging must have spanned the width of the confocal image and had appropriate fluorescent properties to be seen on the photograph.

Another consideration for potential study limitation is the use of control and Th2-predominant AFRS sinonasal tissue sections as a surrogate measure for baseline assessments of epithelial migratory and adherens junction protein levels. As stated in the previous text, the ideal measurement of baseline protein levels following the 24 hour initial cytokine exposure period would be to study *in vitro* sinonasal epithelial layers for protein levels immediately prior to wounding. However, as noted, limitations in available sinonasal epithelial cultures and other resources precluded this type of assessment. Therefore, the control and AFRS sinonasal tissue specimens were employed as a surrogate baseline measure. It is felt that despite potential limitations with this alternative baseline measure, the use of primary sinonasal surgical biopsy specimens across multiple control and Th2-predominant AFRS patients does allow for a translational *in vivo* corollary of epithelial migratory and adherens junction protein expression at a quiescent (non-migrating) state.

Finally, this study suffers from relatively small sample sizes. In ideal experimental conditions, group sizes of 30 or more would satisfy normality assumptions of most statistical measures and allow employment of ANOVA and t-test analyses without violating inherent assumptions. Due to limitations in available sinonasal tissue and the length of time necessary for

mature primary sinonasal epithelial cultures to develop, it was not possible to satisfy group sizes of 30 or greater in this study. Therefore, non-parametric measures were employed for certain statistical analyses and reasons supporting the use of mixed factorial ANOVA have been enumerated in the Methods section. Even with the use of non-parametric statistical analyses, which have inherently less power to detect statistical significance than their parametric counterparts, a number of significant differences were identified in this study.

Like any scientific experiment or clinical trial, the limitations of the study must be considered in the context of the methods and results that are presented. This study has certain potential limitations, but nonetheless, presents interesting and novel results in a field that has been substantially understudied.

CONCLUSIONS

In a translational model of *in vitro* sinonasal epithelial wound healing, Th2 cytokine IL-4 exposure results in reduced sinonasal epithelial wound closure over time and decreased total number of wounds closed compared with sinonasal tissues not exposed to IL-4. In contrast to initial hypotheses, similar impairment in sinonasal epithelial wound healing was not seen under conditions of IL-5 and IL-13 exposure. In fact, wounds under IL-5 and IL-13 exposure more closely mirrored no-cytokine exposure control with respect to healing rates and final number of wounds closed at the completion of experiments. Consistent decreases in sinonasal epithelial wound edge expression of migratory proteins annexin 2 and vinculin, as well as adherens junction protein β-catenin are also seen with IL-4 exposure during active wound healing. These wound edge protein alterations likely contribute to the impairment in sinonasal epithelial wound healing seen under IL-4 exposure conditions.

FUTURE DIRECTIONS

Based upon the results of this study, additional investigations into the mechanisms of sinonasal epithelial wound healing will be pursued. First, *in vitro* sinonasal epithelial wound healing timed studies will be undertaken with cultures of epithelial cells from patients with inflammatory CRS. Preliminary findings indicate that certain epithelial permeability characteristics of the source patient are retained in primary sinonasal epithelial culture, based upon the presence of Th2 inflammatory CRS versus non-inflammatory specimens. These inherent epithelial permeability characteristics are likely to contribute to defects in epithelial migration and wound healing. Further, specifically chosen Th1 and Th2 cytokine combinations will be used to recreate the inflammatory cytokine microenvironment during these *in vitro* sinonasal epithelial wound healing studies, in order to more closely mirror the *in vivo* condition following sinus surgery for inflammatory rhinosinusitis. Finally, additional investigations into the mechanisms for decreased expression of epithelial migratory proteins annexin 2 and vinculin with IL-4 exposure are planned. Taken together, these future studies will progress understanding of pathophysiologic mechanisms underlying impaired and prolonged sinonasal wound healing following sinus surgery for inflammatory rhinosinusitis.

REFERENCES

1. Pleis J, Ward B, and Lucas J. Sumary of health statistics for U.S. adults: National Health Interview Survey, 2009. *National Center for Health Statistics: Vital Health Statistics.* 2010; series 10: number 249.

2. Bhattacharyya N. Comtemporary assessment of the disease burden of sinusitis. *Am J Rhinol Allergy*. 2009:23(4);392-395.

3. Bhattacharyya N. Incremental health care utilization and expenditures for chronic rhinosinusitis in the United States. *Ann Otol Rhinol Laryngol.* 2011;120(7):423-427.

4. Soler ZM, Mace JC, and Smith TL. Symptom-based presentation of chronic rhinosinusitis and symptom-specific outcomes after endoscopic sinus surgery. *Am J Rhinol.* 2008;22(3):297-301.

5. Bhattacharyya N. Ambulatory sinus and nasal surgery in the United States: demographic and perioperative outcomes. *Laryngoscope.* 2010;120(3):635-638.

6. Venkatraman G, Likosky DS, Zhou W, et al. Trends in endoscopic sinus surgery rates in the Medicare population. *Arch Otolaryngol Head Neck Surg*. 2010;136(5):426-430.

7. Albu S and Lucaciu R. Prophylactic antibiotics in endoscopic sinus surgery: a short follow-up study. *Am J Rhinol Allergy*. 2010;24(4):306-309.

8. Cote DW and Wright ED. Trimcinolone-impregnated nasal dressing following endoscopic sinus surgery: a randomized, double-blind, placebo-controlled study. *Laryngoscope*. 2010;120(6):1269-1273.

9. Valentine R, Athanasiadis T, Moratti S, et al. The efficacy of a novel chitosan gel on hemostasis and wound healing after endoscopic sinus surgery. *Am J Rhinol Allergy*. 2010;24(1):70-75.

10. Jorrisen M and Bachert C. Effect of corticoseroids on wound healing after sinus surgery. *Rhinology*. 2009;47(3):280-286.

11. Ramadan HH and Hinerman RA. Smoke exposure and outcome of endoscopic sinus surgery in children. *Otolaryngol Head Neck Surg.* 2002;127(6):546-548.

12. Kim HY, Dhong HJ, Chung SK, et al. Prognostic factors of pediatric endoscopic sinus surgery. *Int J Pediatr Otorhinolaryngol.* 2005;69(11):1535-1539.

13. Atef A, Zeid IA, Qotb M, et al. Effects of passive smoking on ciliary regeneration of nasal mucosa after functional endoscopic sinus surgery in children. *J Laryngol Otol.* 2009;123(1):75-79.

14. Lazard DS, Moore A, Hupertan V, et al. Muco-ciliary differentiation of nasal epithelial cells is decreased after wound healing in vitro. *Allergy*. 2009;64(8):1136-1143.

15. Tan L, Hatzirodos N, and Wormald P-J. Effect of nerve growth factor and keratinocyte growth factor on wound healing of the sinus mucosa. *Wound Repair Regen.* 2008;16(1)108-116.

16. Riechelmann H, Deutschle T, Rozsasi A, et al. Nasal biomarker profiles in acute and chronic rhinosinusitis. *Clin Exp Allergy*. 2005;35(9):1186-1191.

17. van Zele T, Claeys S, Gavaert P, et al. Differentiation of chronic sinus diseases by measurement of inflammatory mediators. *Allergy*. 2006;61(11):1280-1289.

18. Batemen ND, Fahy C, and Woolford TJ. Nasal polyps: still more questions than answers. *J Laryngol Otol.* 2003;117(1);1-9.

19. Drake-Lee AB and McLaughlin P. Clinical symptoms, free histamine and IgE in nasal polyps. *Int Arch Allergy Appl Immunol.* 1982;69(3):268-271.

20. Hamilos DL, Leung DY, Wood R, et al. Chronic hyperplastic sinusitis: association of tissue eosinophilia and cytokine mRNA expression of granulocyte-macrophage colony-stimulating factor and interleukin-3. *J Allergy Clin Immunol.* 1993;92(1):39-48.

21. Durham SR, Ying S, Varney VA, et al. Cytokine messenger mRNA expression for IL-3, IL-4, IL-5, and granulocyte-macrophage colony-stimulating factor after local allergen provocation: relationship to tissue eosinophilia. *J Immunol.* 1992;48(8):2390-2394.

22. Allen JS, Eisma R, Leonard G, et al. Interleukin-3, interleukin-5, and granulocyte-macrophage colony-stimulating factor expression in nasal polyps. *Am J Otolaryngol.* 1997;18(4):239-246.

23. Allen JS, Eisma R, Leonard G, et al. Interleukin-8 expression in human nasal polyps. *Otolaryngol Head Neck Surg.* 1997;117(5):535-541.

24. Bachert C, Wagenmann M, Hauser U, et al. IL-5 synthesis is upregulated in human nasal polyp tissue. *J Allergy Clinical Immunol.* 1997;99(6):837-842.

25. Elovic A, Wong DT, Weller PF, et al. Expression of transforming growth factors alpha and beta-1 messenger RNA and product by eosinophils in nasal polyps. *J Allergy Clin Immunol.* 1994;93(5):864-869.

26. Jahnsen FL, Haraldsen G, Aanesen JP, et al. Eosinophil infiltration is related to increased expression of vascular cell adhesion molecule-1 in nasal polyps. *Am J Resp Cell Mol Biol.* 1995;12(6):624-632.

27. Coste A, Brugel L, Maître B. et al. Inflammatory cells as well as epithelial cells in nasal polyps express vascular endothelial growth factor. *Eur Resp J.* 2000;15(2):367-372.

28. Borthwick LA, McIlroy EI, Gorowiec MR. et al. Inflammation and epithelial to mesenchymal transition in lung transplant recipients: role in dysregulated epithelial wound repair. *Am J Transplant.* 2010;10(3):496-509.

29. Ahdieh M, Vandenbos T, and Youakim A. Lung epithelial barrier function and wound healing are decreased by IL-4 and IL-13 and enhanced by IFN-gamma. *Am J Physiol Cell Physiol*. 2001;281(8):C2029-2038.

30. Leitch VD, Strudwick XL, Matthaei KI, et al. IL-5 overexpressing mice exhibit eosinophilia and altered wound healing through mechanisms involving prolonged inflammation. *Immunol Cell Biol*. 2009;87(2):131-140.

31. Schäffer M, Weimer W, Wider S, et al. Differential expression of inflammatory mediators in radiation-impaired wound heaing. *J Surg Res.* 2002;107(1):93-100.

32. Henry G and Garner WL. Inflammatory mediators in wound healing. *Surg Clin North Am.* 2003;83(3):483-507.

33. Babbin BA, Parkos CA, Mandell KJ, et al. Annexin 2 regulates intestinal epithelial cell spreading and wound closure through Rho-related signaling. *Am J Pathol*. 2007;170(3):951-966.

34. Nusrat A, Parkos CA, Liang TW, et al. Neutrophil migration across model intestinal epithelia: monolayer disruption and subsequent events in epithelial repair. *Gastroenterology*. 1997;113(5):1489-1500.

35. Kirshner J, Schumann D, and Shively JE. CEACAM1, a cell-cell adhesion molecule, directly associates with annexin II in a three-dimensional model of mammary morphogenesis. *J Biol Chem.* 2003;278(50):50338-50345.

36. Goldmann WH and Ingber DE. Intact vinculin protein is required for control of cell shape, cell mechanics, and rac-dependent lamellipodia formation. *Biochem and Biophys Res Comm.* 2002;290(2):749-755.

37. Nermut MV, Green NM, Eason P, et al. Electron microscopy and structural model of human fibronectin receptor. *EMBO J.* 1988;7(13):4093-4099.

38. Chen H, Paradies NE, Fedor-Chaiken M, et al. E-cadherin mediates adhesion and suppresses cell motility via direct mechanisms. *J Cell Science*. 1997;110(3):345-356.

39. Stojadinovic O, Brem H, Vouthounis C, et al. Molecular pathogenesis of chronic wounds: the role of beta-catenin and c-myc in the inhibition and epithelialization and wound healing. *Am J Pathol.* 2005;167(1):59-69.

40. *Entrez Gene.* December 4, 2011. http://www.ncbi.nih.gov/sites/entrez (accessed December 9, 2011).

41. Bent JP and Kuhn FA. Diagnosis of allergic fungal sinusitis. *Otolaryngol Head Neck Surg.* 1994;111(5):580-588.

42. Lane AP, Saatian B, Yu XY, et al. mRNA for genes associated with antigen presentation are expressed by human middle meatal epithelial cells in culture. *Laryngoscope*. 2004;114(10):1827-1832.

43. Hawker KM, Johnson PR, Hughes JM, et al. Interleukin-4 inhibits mitogen-induced proliferation of human airway smooth muscle cells in culture. *Am J Physiol*. 1998;275(3):L469-477.

44. Costa GG, Silva RM, Franco-Penteado CF, et al. Interactions between eotaxin and interleukin-5 in the chemotaxis of primed and non-primed human eosinophils. *Eur J Pharmacol*. 2007;566(1-3);200-205.

45. Chapekar MS and Glazer RI. Effects of human immune interferon on cell viability, (2',5') oligoadenylate synthesis, and polyamine-dependent protein phosphorylation in human colon carcinoma cells in vitro. *Cancer Res*. 1984;44(5):2144-2149.

46. Tang KT, Braverman LE, and DeVito WJ. Tumor necrosis factor-alpha and interferon-gamma modulate gene expression of type I 5'-deiodinase, thyroid peroxidase, and thyroglobulin in FRTL-5 rat thyroid cells. *Endocrinology*. 1995;136(3):881-888.

47. Nagai S, Hashimoto S, Yamashita T, et al. Comprehensive gene expression profile of human activated Th1- and Th2-polarized cells. *Int Immunol*. 2001;13(3):367-376.

48. Zuckerman JD, Lee WY, DelGaudio JM, et al. Pathophysiology of nasal polyposis: the role of desmosomal junctions. *Am J Rhinol*. 2008;22(6):589-97.

49. Rogers GA, Den Beste K, Parkos CA, et al. Epithelial tight junction alterations in nasal polyposis. *Int Forum Allergy Rhinol*. 2011;1(1):50-54.

FIGURE 1 – PROPOSED CAUSAL DIAGRAM. This figure depicts the causal diagram postulated in this study. Dashed arrows indicate potential confounding relationships between baseline protein levels and the exposure and outcome measures.

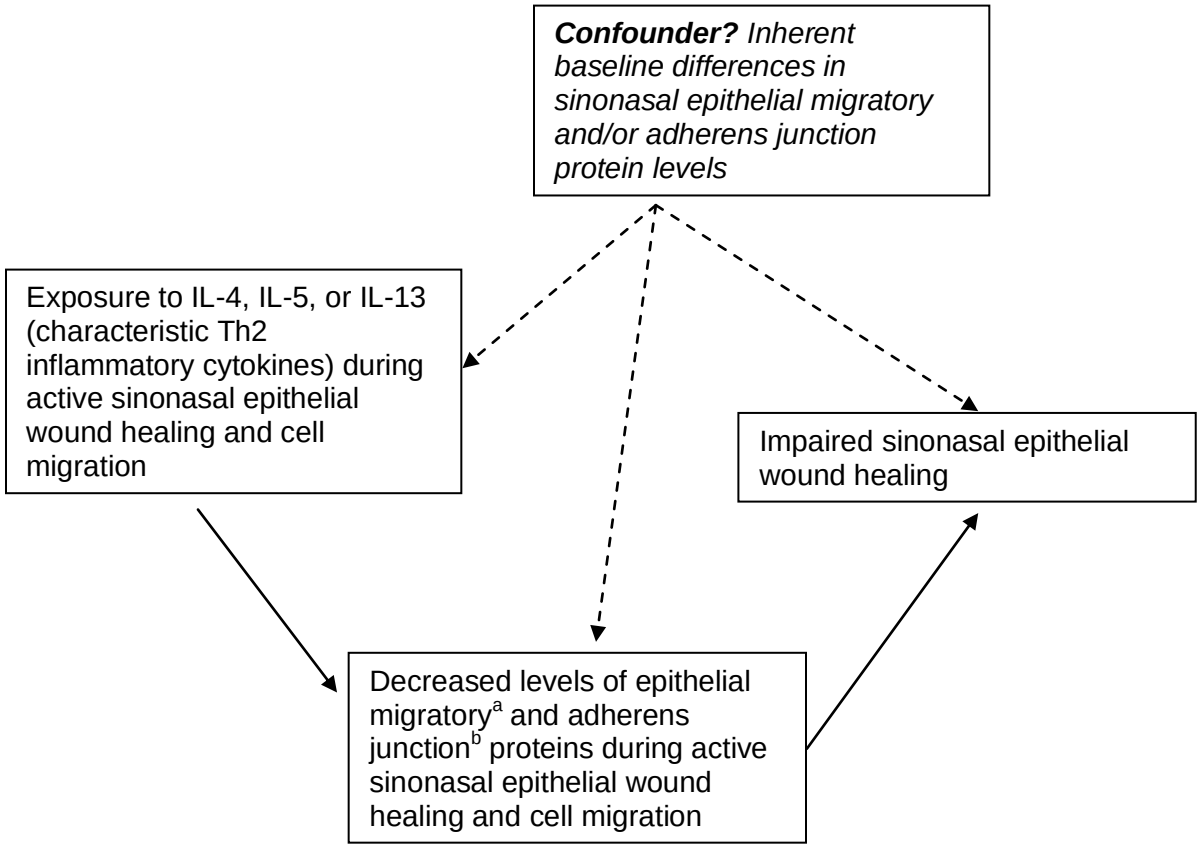

a. Epithelial migratory proteins:

Annexin 2

Vinculin

β1-integrin

b. Adherens junction proteins:

E-cadherin

β-catenin

FIGURE 2 – ELECTRON MICROSCOPY IMAGES OF CILIATED PRIMARY SINONASAL EPITHELIAL CELL CULTURE. Transmission (a) and scanning (b) electron microscopy images of primary sinonasal epithelial cell culture grown from a non-inflammatory control patient

(a)

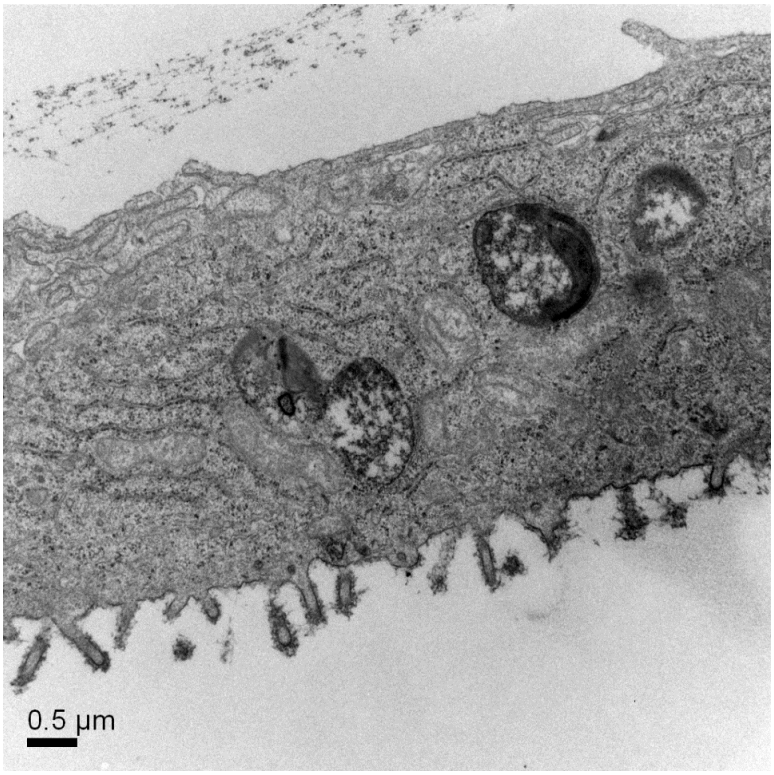

(b)

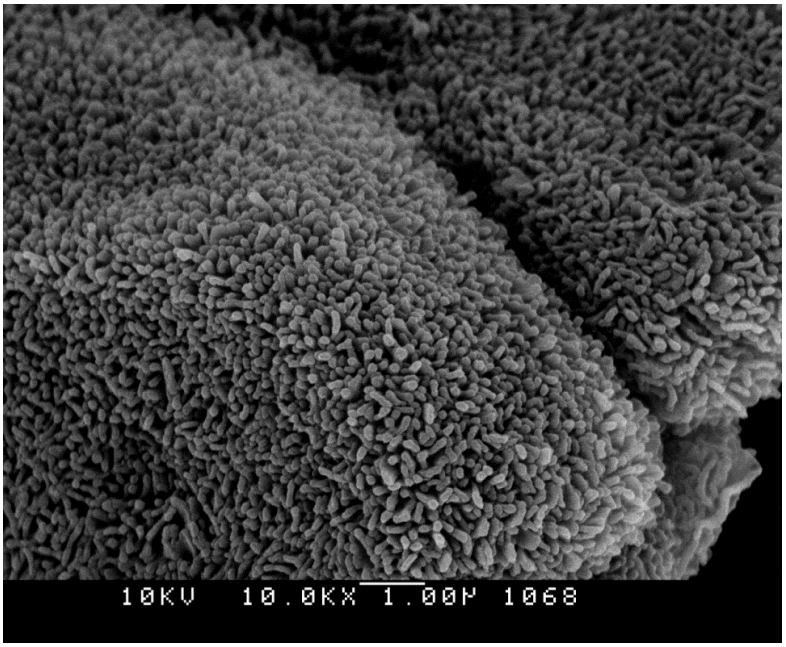

FIGURE 3 – EXAMPLE OF WOUND AREA CALCULATION DURING TIMED SINONASAL EPITHELIAL WOUND CLOSURE EXPERIMENT

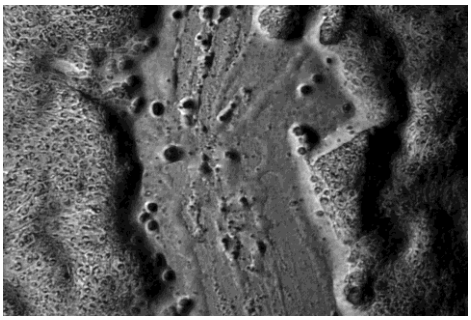

(a1) Initial wound

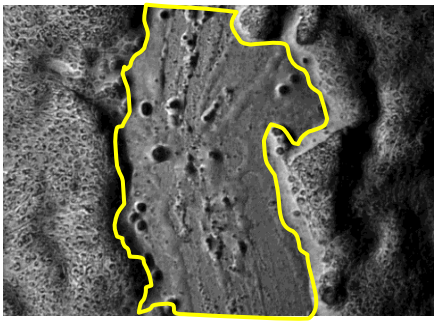

(a2) Initial wound with area outline

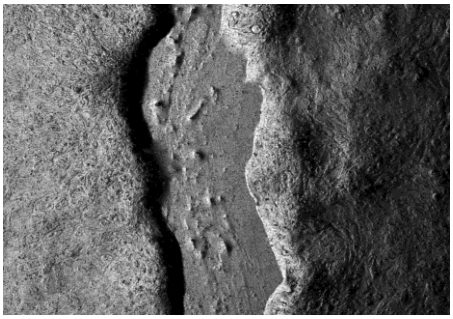

(b1) 12 hours post-wounding

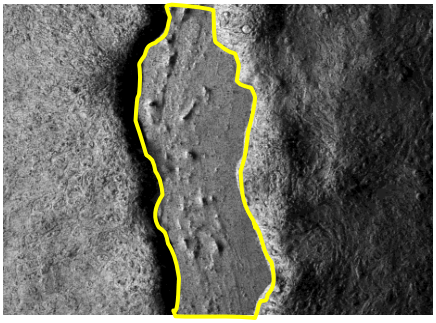

(b2) 12 hours post wounding with area outline

(c1) 24 hours post-wounding

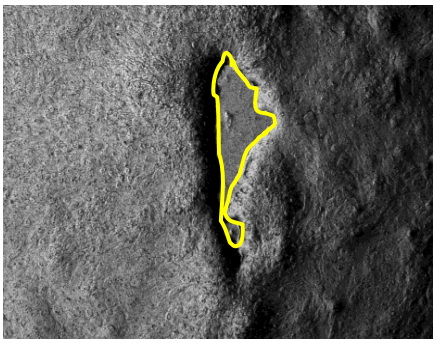

(c2) 24 hours post wounding with area outline

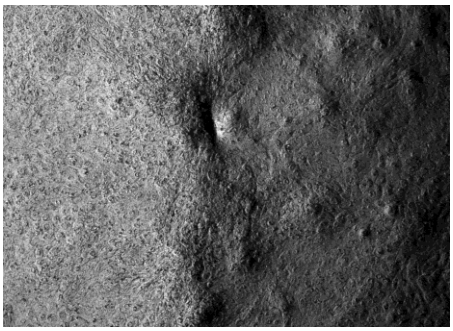

(d1) 36 hours post-wounding

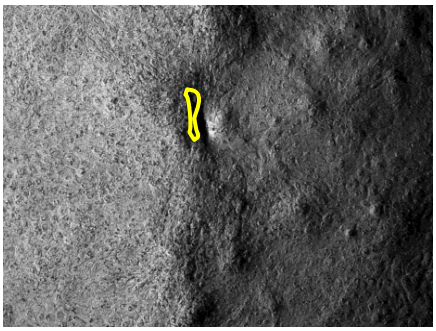

(d2) 36 hours post wounding with area outline

Microscopic photograph of initial wound and 12-36 hour example photographs of the same wound during spontaneous closure. (a2-d2) Microscopic photographs of initial wound and 12-36 hour wounds with example wound edge outline overlays. Area of each wound was calculated with ImageJ image analysis program.

FIGURE 4 – EXAMPLE OF SINONASAL EPITHELIAL WOUND EDGE PIXEL ANALYSIS

(a)

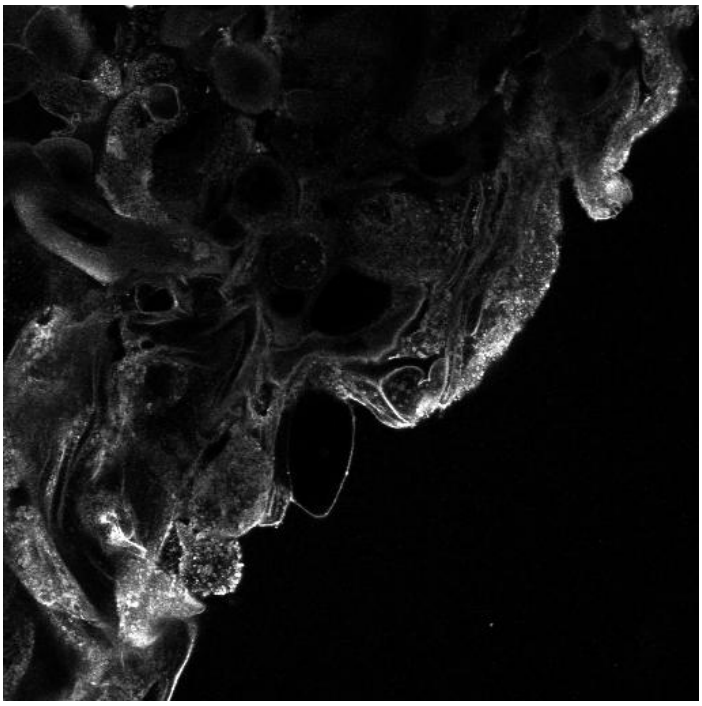

(b)

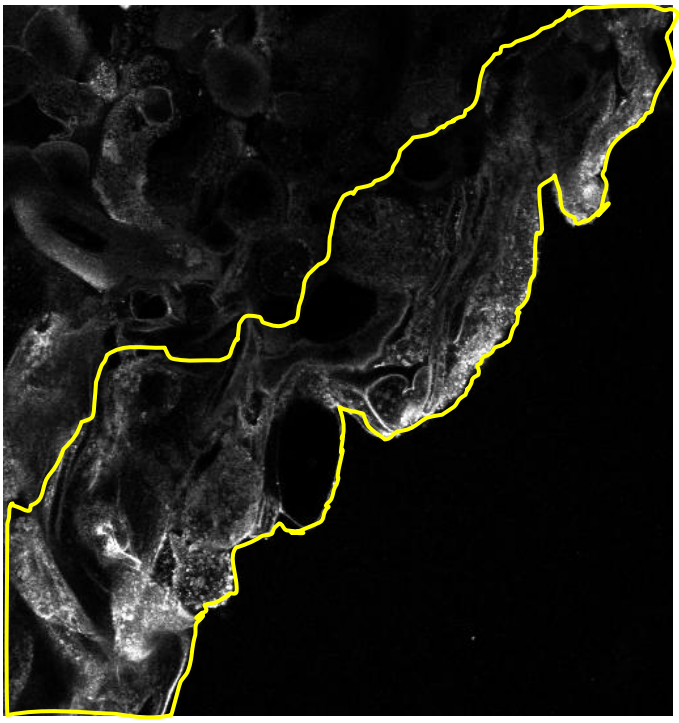

(a) Sinonasal epithelial wound edge confocal microscopy image. All images for experiments in this series were taken at 40X magnification. Images are converted to grayscale for pixel intensity analysis. Immunofluorescence staining was performed with anti-annexin 2 antibody in this image. (b) Approximately 2 cell layers at wound edge are outlined with image analysis software. Pixel density is calculated per area of wound edge for each confocal microscopy image.

FIGURE 5 – EXAMPLE OF PROTEIN IMMUNOFLUORESCENCE STAINING PIXEL DENSITY CALCULATIONS PER EPITHELIAL AREA IN SINONASAL TISSUE BIOPSIES

(a)

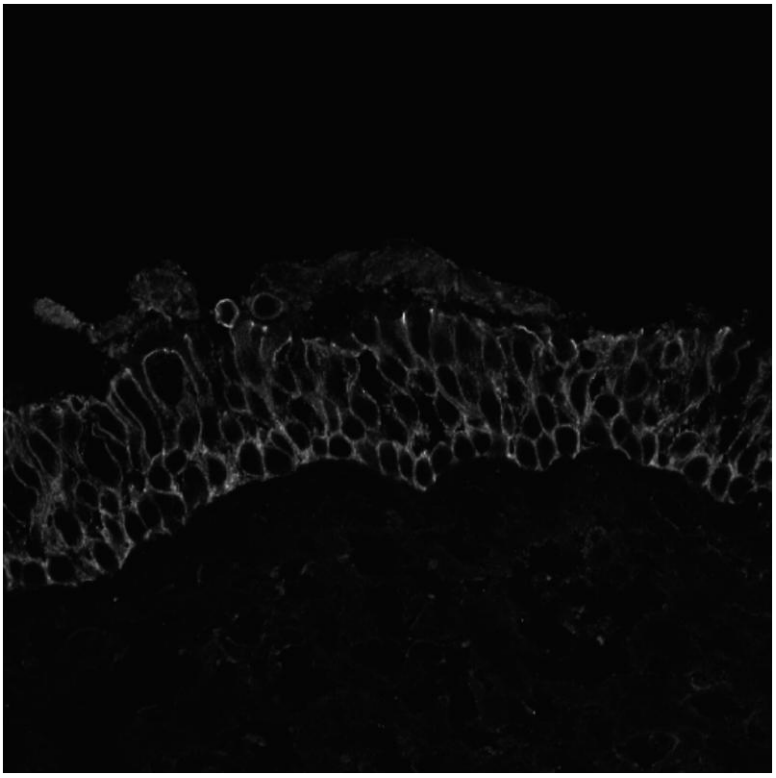

(b)

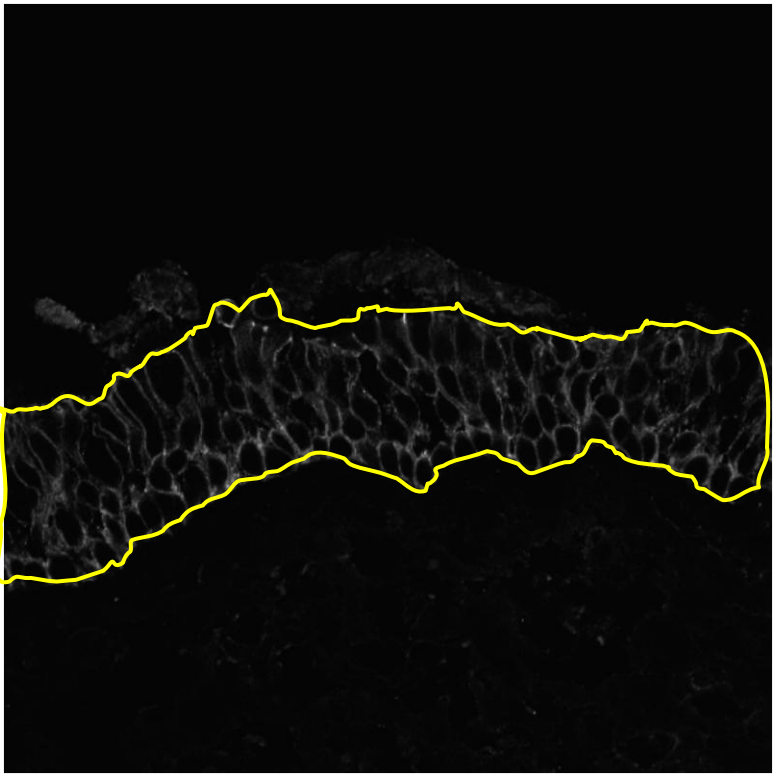

Sinonasal biopsy immunofluorescent images are captured by confocal microscopy. All images for experiments in this series were taken at 40X magnification. Images are converted to grayscale for pixel intensity analysis (a). Epithelium is identified and outlined with image analysis software (b). Pixel density within the epithelial outline is divided by the area of the outlined epithelium.

TABLE 1 – PERCENTAGE WOUND CLOSURE BY CYTOKINE EXPOSURE

Time point	Mean Percentage Wound Closure	Standard Deviation	Standard Error of Mean
4 hrs.			
Control	14.53	5.57	1.61
IFNγ-TNFα	4.30	6.55	1.89
IL-4	6.17	4.70	1.36
IL-5	6.84	5.39	1.56
IL-13	7.71	4.16	1.20
8 hrs.			
Control	30.77	12.05	3.48
IFNγ-TNFα	8.33	10.85	3.13
IL-4	13.77	8.06	2.33
IL-5	22.26	11.57	3.34
IL-13	19.16	9.15	2.64
12 hrs.			
Control	43.58	17.51	5.05
IFNγ-TNFα	15.90	13.81	3.99
IL-4	19.66	13.54	3.91
IL-5	37.42	18.41	5.31
IL-13	31.48	18.80	5.43
16 hrs.			
Control	55.77	14.88	4.30
IFNγ-TNFα	32.74	17.56	5.07
IL-4	34.66	23.44	6.77
IL-5	54.17	19.01	5.49
IL-13	51.97	24.98	7.21
20 hrs.			
Control	72.76	16.25	4.69
IFNγ-TNFα	47.22	20.12	5.81
IL-4	45.07	24.77	7.15
IL-5	68.00	18.06	5.21
IL-13	62.43	23.83	6.88
24 hrs.			
Control	89.01	12.97	3.74
IFNγ-TNFα	61.24	21.31	6.15
IL-4	58.37	21.76	6.29
IL-5	89.11	12.57	3.63
IL-13	77.87	17.82	5.15
28 hrs.			
Control	93.32	9.63	2.78
IFNγ-TNFα	78.56	17.10	4.94
IL-4	69.36	22.15	6.40
IL-5	95.93	6.77	1.96
IL-13	88.20	14.54	4.20
32 hrs.			
Control	97.09	5.48	1.58
IFNγ-TNFα	88.46	13.13	3.79
IL-4	77.68	19.78	5.71
IL-5	98.56	3.58	1.03
IL-13	93.82	10.23	2.95
36 hrs.			
Control	98.40	3.43	0.99
IFNγ-TNFα	96.50	5.99	1.73
IL-4	85.02	18.46	5.33
IL-5	99.38	2.14	0.62
IL-13	95.03	7.58	2.19

This table demonstrates mean percentage wound closure, standard deviation, and standard error of the mean for each cytokine exposure group at each post-wounding time point (n = 12 wounds per cytokine exposure group). For each cytokine exposure by time group, a measure of normality, skewness statistic divided by the standard error of the skewness statistic, was also performed (data not presented in table). By convention, values of this normality measure of 2 or less are considered relatively normally distributed. With few exceptions, the vast majority of sample value sets are normally distributed (value < 2) until the 32 and 36 hour post-wounding time points. It is not surprising that these later post-wounding time points have skewed distributions, as many of the wounds had achieved 100% closure by these time points.

Significant findings:

Main effect of time ($p<0.001$)

No-cytokine control

vs. IFNγ-TNFα ($p=0.005$)

vs. IL-4 ($p=0.001$)

IFNγ-TNFα

vs. IL-4 ($p=0.005$)

vs. IL-5 ($p=0.023$)

Time by cytokine exposure interaction ($p<0.001$). See TABLE 2 for individual significant differences.

FIGURE 6 – REPEATED MEASURES *IN VITRO* SINONASAL EPITHELIAL WOUND HEALING STUDY FOLLOWING 24-HOUR CYTOKINE EXPOSURE

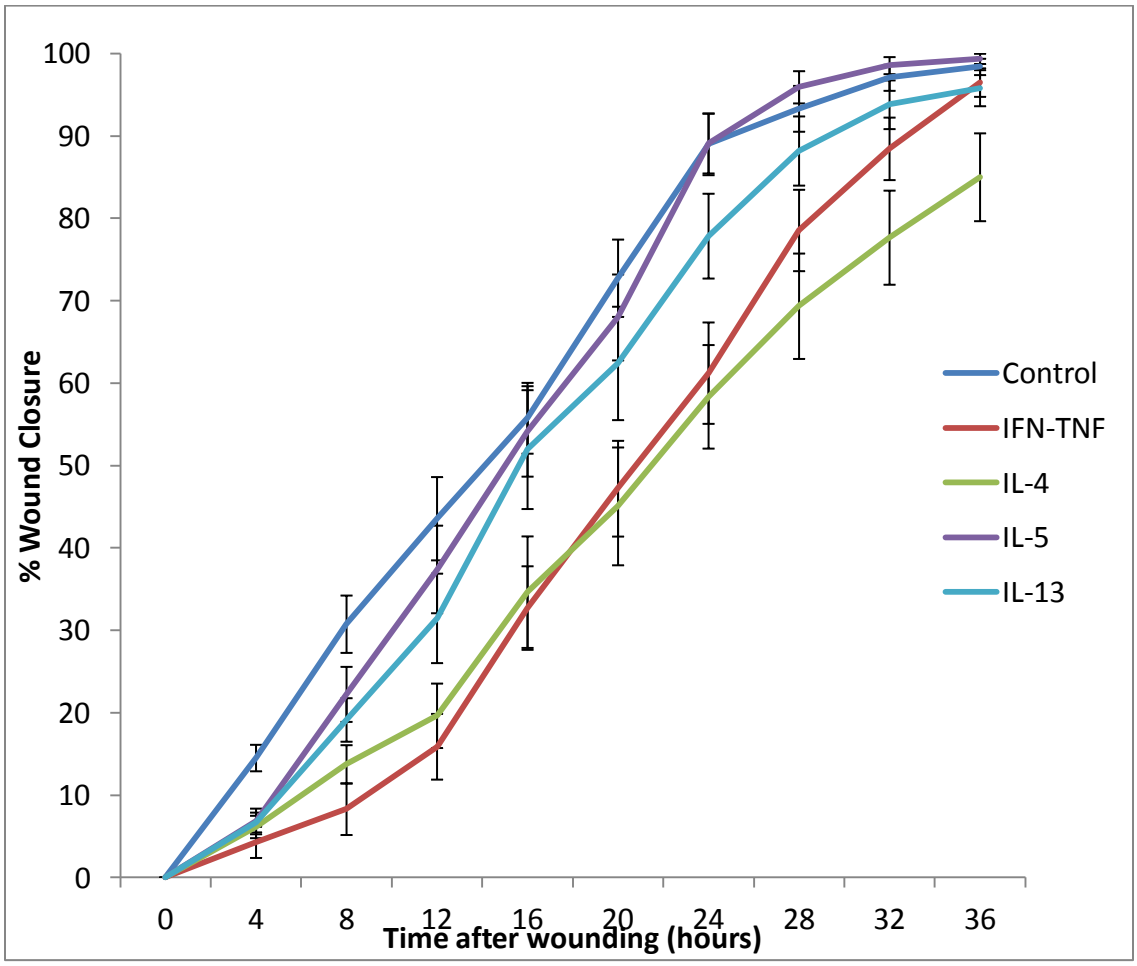

This chart graphically represents the mean percentage wound closure of sinonasal epithelial wound closure under 5 cytokine exposure conditions for the 36-hours post-wounding timecourse. Cytokine exposure groups are denoted by colored lines. Error bars represent standard error of the mean.

TABLE 2 – TUKEY POST-HOC ANALYSIS OF GROUP DIFFERENCES BY CYTOKINE

		Vs. Control	Vs. IFNγ-TNFα	Vs. IL-4	Vs. IL-5	Vs. IL-13
		Mean difference	Mean difference	Mean difference	Mean difference	Mean difference
Timepoint	Mean					
4 hrs.						
Control	14.53	----	10.23	8.36	7.69	6.82
IFNγ-TNFα	4.30	10.23	----	1.87	2.54	3.41
IL-4	6.17	8.36	1.87	----	0.67	1.54
IL-5	6.84	7.69	2.54	0.67	----	0.87
IL-13	7.71	6.82	3.41	1.54	0.87	----
8 hrs.						
Control	30.77	----	***22.44****	***17.00****	8.51	11.61
IFNγ-TNFα	8.33	***22.44****	----	5.44	***13.93****	10.83
IL-4	13.77	***17.00****	5.44	----	8.49	5.39
IL-5	22.26	8.51	***13.93****	8.49	----	3.10
IL-13	19.16	11.61	10.83	5.39	3.10	----
12 hrs.						
Control	43.58	----	***27.68****	***23.92****	6.16	12.10
IFNγ-TNFα	15.90	***27.68****	----	3.76	***21.52****	***15.58****
IL-4	19.66	***23.92****	3.76	----	***17.76****	11.82
IL-5	37.42	6.16	***21.52****	***17.76****	----	5.94
IL-13	31.48	12.10	***15.58****	11.82	5.94	----
16 hrs.						
Control	55.77	----	***23.03****	***21.11****	1.60	3.80
IFNγ-TNFα	32.74	***23.03****	----	1.92	***21.43****	***19.23****
IL-4	34.66	***21.11****	1.92	----	***19.51****	***17.31****
IL-5	54.17	1.60	***21.43****	***19.51****	----	2.20
IL-13	51.97	3.80	***19.23****	***17.31****	2.20	----
20 hrs.						
Control	72.76	----	***25.54****	***27.69****	4.76	10.33
IFNγ-TNFα	47.22	***25.54****	----	2.15	***20.78****	***15.21****
IL-4	45.07	***27.69****	2.15	----	***22.93****	***17.36****
IL-5	68.00	4.76	***20.78****	***22.93****	----	5.57
IL-13	62.43	10.33	***15.21****	***17.36****	5.57	----
24 hrs.						
Control	89.01	----	***27.77****	***30.64****	0.10	11.14
IFNγ-TNFα	61.24	***27.77****	----	2.87	***27.87****	***16.63****
IL-4	58.37	***30.64****	2.87	----	***30.74****	***19.50****
IL-5	89.11	0.10	***27.87****	***30.74****	----	11.24
IL-13	77.87	11.14	***16.63****	***19.50****	11.24	----
28 hrs.						
Control	93.32	----	***14.76****	***23.96****	2.61	5.12
IFNγ-TNFα	78.56	***14.76****	----	9.20	***17.37****	9.64
IL-4	69.36	***23.96****	9.20	----	***26.57****	***18.84****
IL-5	95.93	2.61	***17.37****	***26.57****	----	7.73
IL-13	88.20	5.12	9.64	***18.84****	7.73	----
32 hrs.						
Control	97.09	----	8.63	***19.41****	1.47	3.27
IFNγ-TNFα	88.46	8.63	----	10.78	10.10	5.36
IL-4	77.68	***19.41****	10.78	----	***20.70****	***16.14****
IL-5	98.56	1.47	10.10	***20.70****	----	4.74
IL-13	93.82	3.27	5.36	***16.14****	4.74	----
36 hrs.						
Control	98.40	----	1.90	***13.38****	0.98	3.37
IFNγ-TNFα	96.50	1.90	----	11.48	2.88	1.47
IL-4	85.02	***13.38****	11.48	----	***14.36****	10.01
IL-5	99.38	0.98	2.88	***14.36****	----	4.35
IL-13	95.03	3.37	1.47	10.01	4.35	----

This table demonstrates individual group differences for mean percent wound healed at each post-wounding time point. Overall time by cytokine exposure group interaction significance level for repeated measures ANOVA is $p<0.001$. Significant differences identified by Tukey post-hoc analysis are noted by an asterisk. Mean difference greater than 12.67 was considered significant based upon the sample number per group ($n = 12$) and degrees of freedom (larger than 240).

FIGURE 7 – REPEATED MEASURES *IN VITRO* SINONASAL EPITHELIAL WOUND HEALING STUDY FOLLOWING 24-HOUR CYTOKINE EXPOSURE – NO-CYTOKINE CONTROL, IFNγ-TNFα, AND IL-4 ONLY

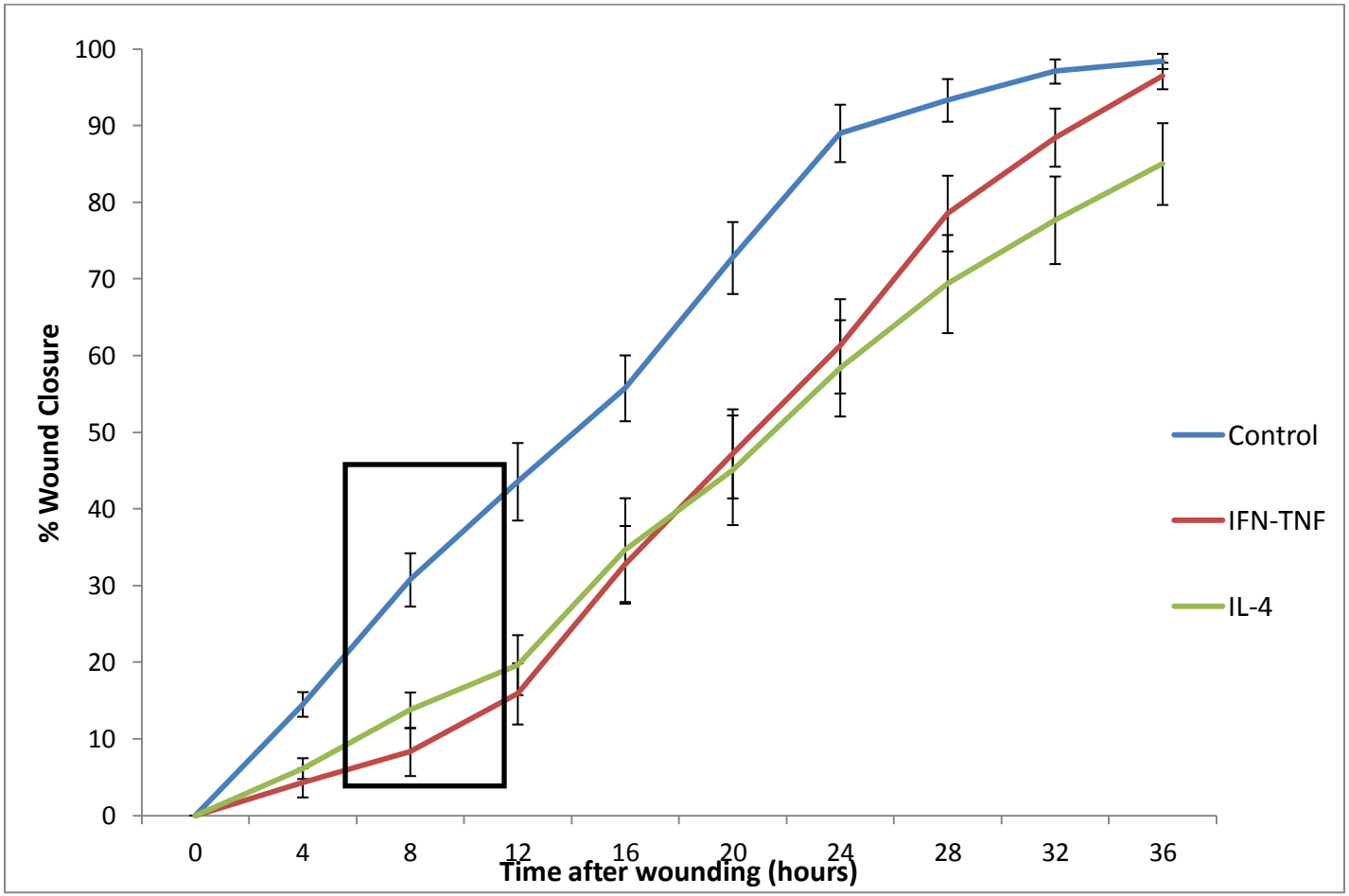

This chart graphically represents the mean percent wound closure of sinonasal epithelial wound closure under cytokine exposure conditions for the 36-hours post-wounding timecourse. Cytokine exposure groups are denoted by colored lines. For better visualization of Th2 cytokine IL-4 versus no-cytokine and IFNγ-TNFα controls, IL-5 and IL-13 lines have been removed. Error bars represent standard error of the mean. A black box has been inserted to highlight the 8-12 hour post-wounding timeframe. Within this timeframe, the rate of wound closure is graphically different amongst cytokine groups. Based upon this finding, the 10-hour post-wounding time point was chosen for additional study of epithelial migratory and adherens junction protein differences during active wound healing amongst cytokine exposure groups.

TABLE 3 – IMMUNOFLUORESCENCE STAINING PIXEL DENSITY ANALYSIS FROM *IN VITRO* SINONASAL EPITHELIAL WOUND HEALING STUDIES

Protein	Inflammatory condition	N per group	Mean pixel density per epithelium area	Median pixel density per epithelium area	Standard deviation	95% confidence interval	Range	Kruskall Wallis p-value
Annexin 2	Control	9	57.50	58.04	13.81	(48.48, 66.52)	41.71-85.27	***0.013****
	IFNγ-TNFα	9	43.17	35.79	23.88	(27.57, 58.77)	19.20-92.18	
	IL-4	10	34.73	35.71	11.57	(27.56, 41.90)	12.04-50.20	
Vinculin	Control	9	61.24	67.96	17.53	(49.79, 72.69)	24.20-76.40	***0.002****
	IFNγ-TNFα	8	29.61	26.07	13.74	(20.09, 39.13)	12.41-52.97	
	IL-4	9	29.96	29.84	9.00	(24.08, 35.84)	13.44-40.65	
β1-integrin	Control	8	13.83	11.83	6.96	(8.97, 18.69)	7.65-26.89	0.325
	IFNγ-TNFα	8	9.96	7.03	6.52	(5.44, 14.48)	4.17-21.42	
	IL-4	9	11.44	10.07	4.92	(8.22, 14.66)	5.61-22.48	
E-cadherin	Control	8	20.34	20.43	6.47	(15.86, 24.82)	12.14-32.99	***0.003****
	IFNγ-TNFα	10	9.94	10.44	4.63	(7.07, 12.81)	3.42-19.69	
	IL-4	10	14.98	12.71	5.88	(11.34, 18.62)	9.28-25.79	
β-catenin	Control	9	19.13	16.00	6.43	(14.93, 23.33)	13.01-32.75	***0.009****
	IFNγ-TNFα	8	25.86	24.20	9.36	(19.37, 32.35)	15.04-34.94	
	IL-4	8	13.81	12.70	5.46	(10.03, 17.59)	7.49-24.20	

This table demonstrates the numerical results of the pixel intensity analyses on *in vitro* cytokine-exposure wound healing studies. Statistical significance identified across all three cytokine exposure groups, as assessed by Kruskall-Wallis analysis, is noted in the far right column. Protein groups with statistically significant differences amongst cytokine exposure conditions are denoted by an asterisk (*). These results are consistent with the hypothesis that cytokine-exposed actively healing epithelial wounds will show decreases in epithelial migratory and adherens junction proteins based on cytokine exposure, given that we have shown IFNγ-TNFα and IL-4 exposed wounds to be closing at a slower rate.

FIGURE 8 – PIXEL DENSITY ANALYSIS FROM CYTOKINE-EXPOSURE WOUND HEALING STUDIES

(a) Annexin 2

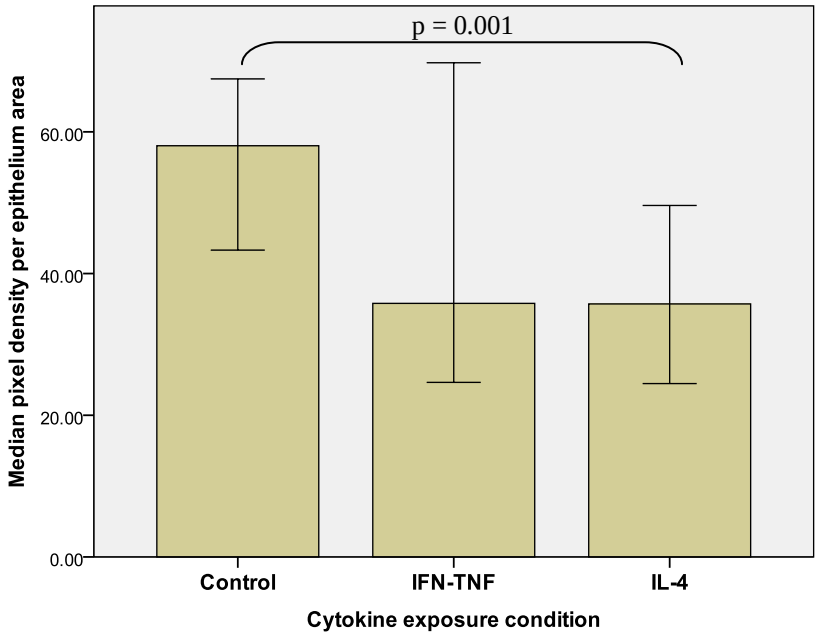

Control: N = 9
IFNγ-TNFα: N = 9
IL-4: N = 10

Kruskall-Wallis:
p = 0.013

(b) Vinculin

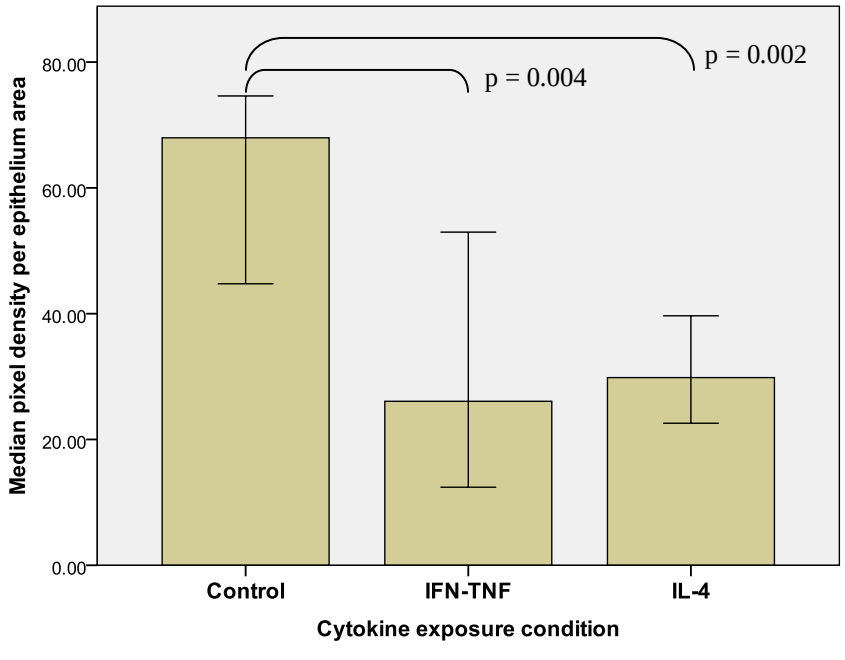

Control: N = 9
IFNγ-TNFα: N = 8
IL-4: N = 9

Kruskall-Wallis:
p = 0.002

(c) β1-integrin

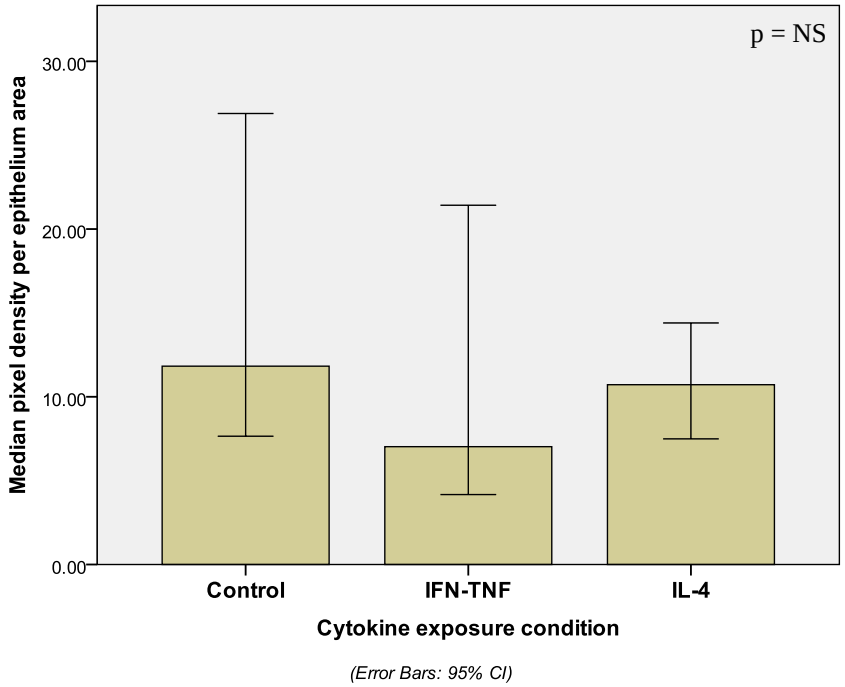

Control: N = 8
IFNγ-TNFα: N = 8
IL-4: N = 9

Kruskall-Wallis:
p = 0.325

(d) E-cadherin

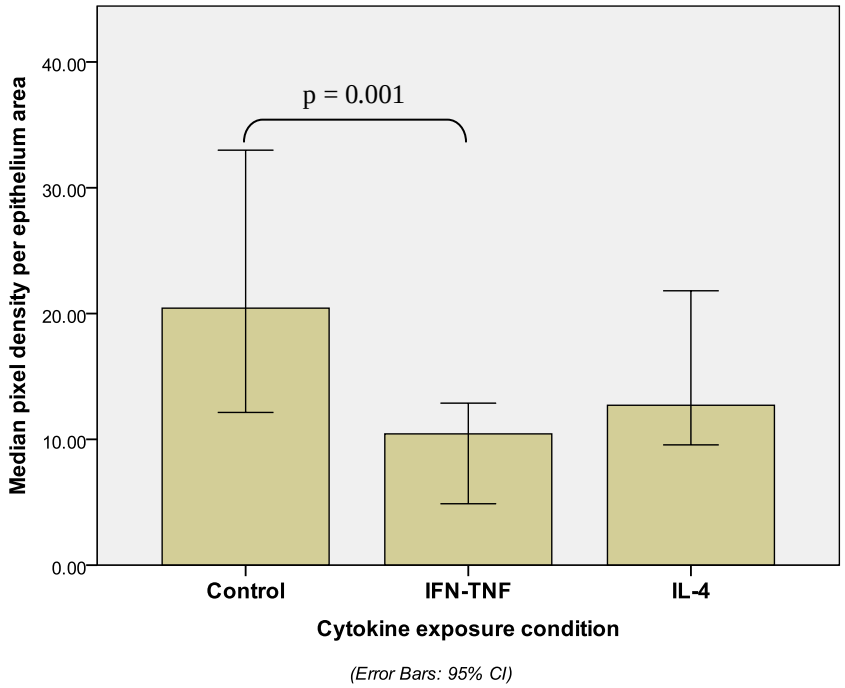

Control: N = 8
IFNγ-TNFα: N = 10
IL-4: N = 10

Kruskall-Wallis:
p = 0.003

(e) β-catenin

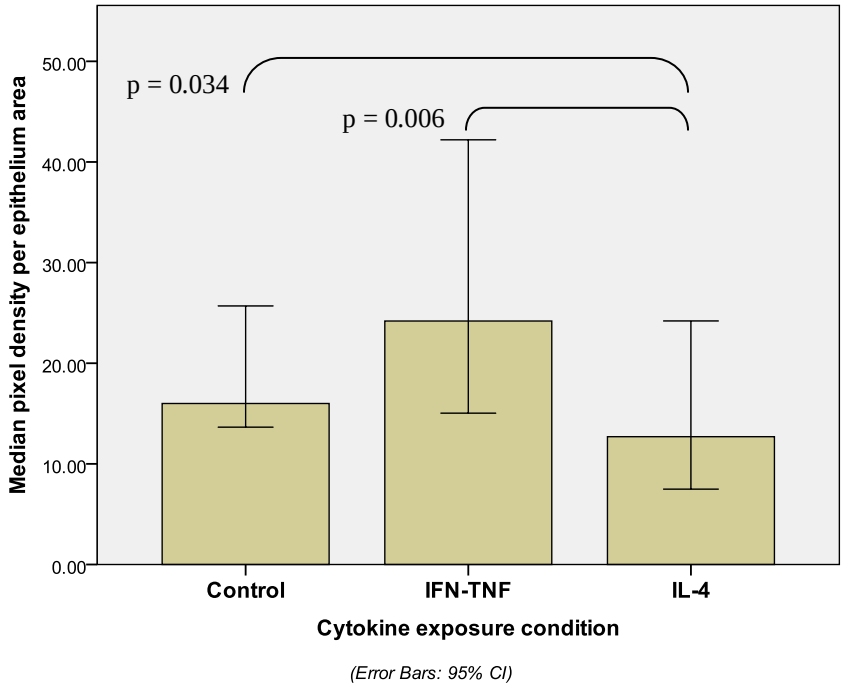

Control: N = 9
IFNγ-TNFα: N = 8
IL-4: N = 8

Kruskall-Wallis:
p = 0.009

Graphs a-e depict pixel density analysis from immunofluorescence images taken at approximately 10 hours post-wounding during *in vitro* cytokine exposure sinonasal wound healing studies. Median ± 95% confidence interval protein intensity is demonstrated by cytokine exposure condition. Brackets in each graph demonstrate statistical significance between cytokine exposure groups, as determined by post-hoc testing following Kruskall-Wallis analysis.

FIGURE 9 – WESTERN IMMUNOBLOT ANALYSIS OF 10 HOUR POST-WOUNDING PROTEIN CHANGES IN *IN VITRO* CYTOKINE-EXPOSED SINONASAL EPITHELIAL WOUND HEALING ASSAY

(a) Annexin 2

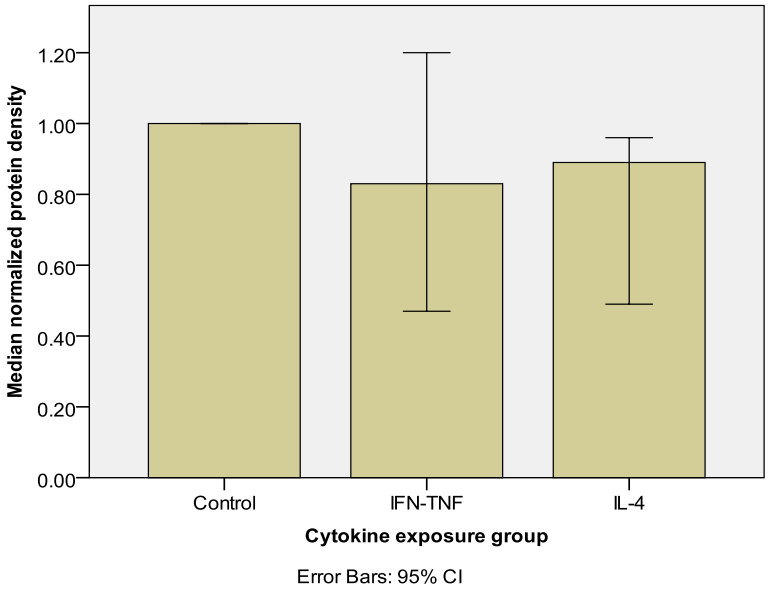

N = 3 experiments

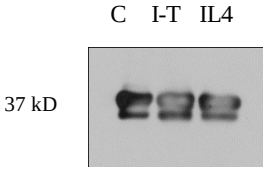

(b) Vinculin

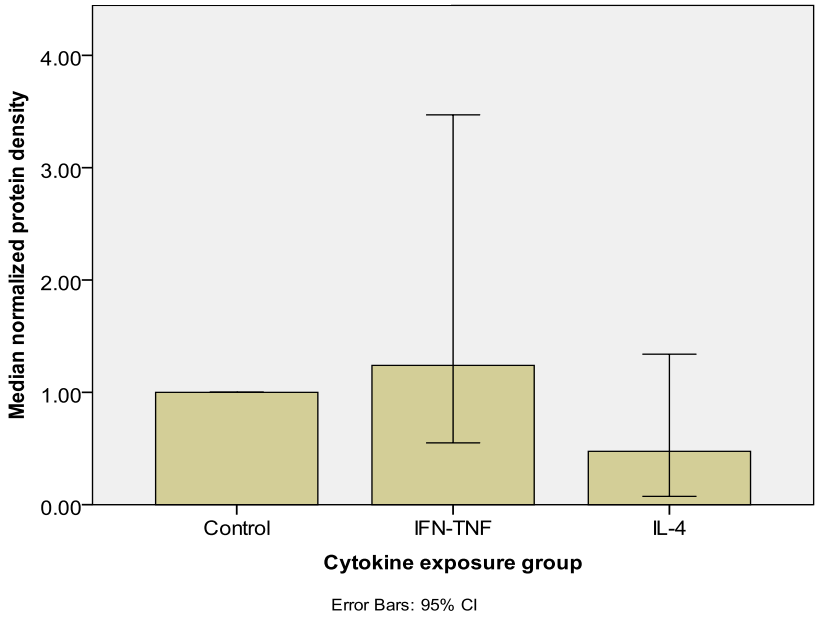

N = 4 experiments

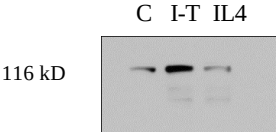

(c) β1-integrin

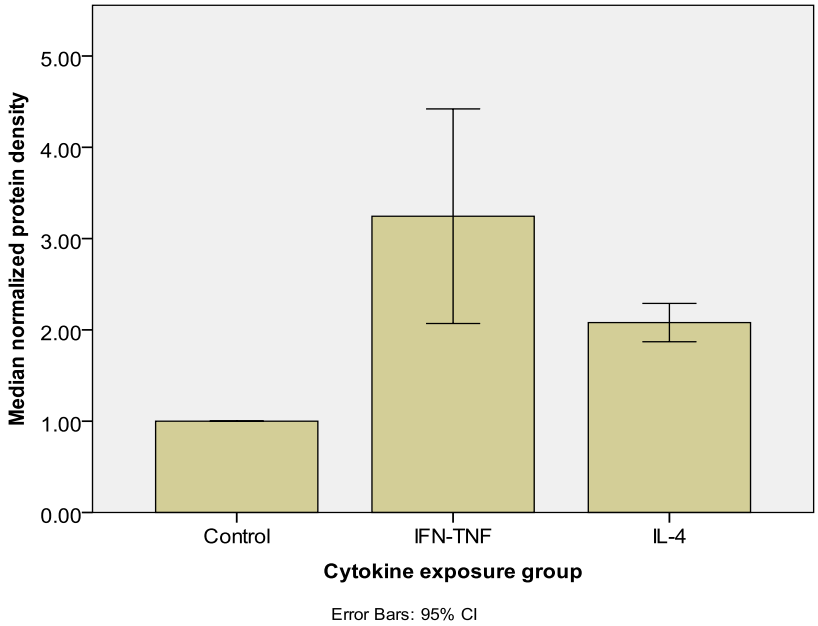

N = 2 experiments

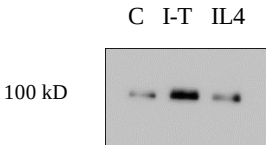

(d) E-cadherin

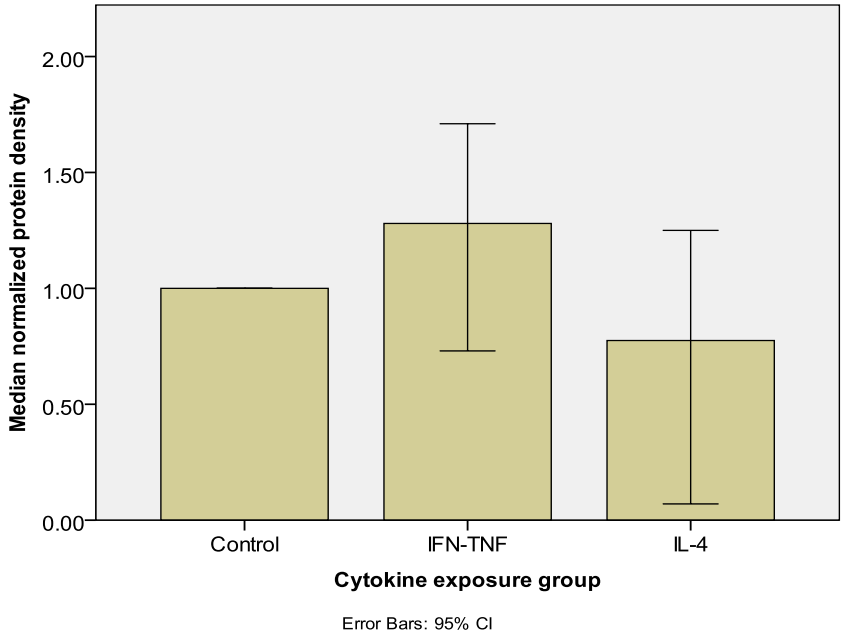

N = 4 experiments

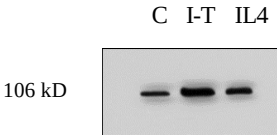

(e) β-catenin

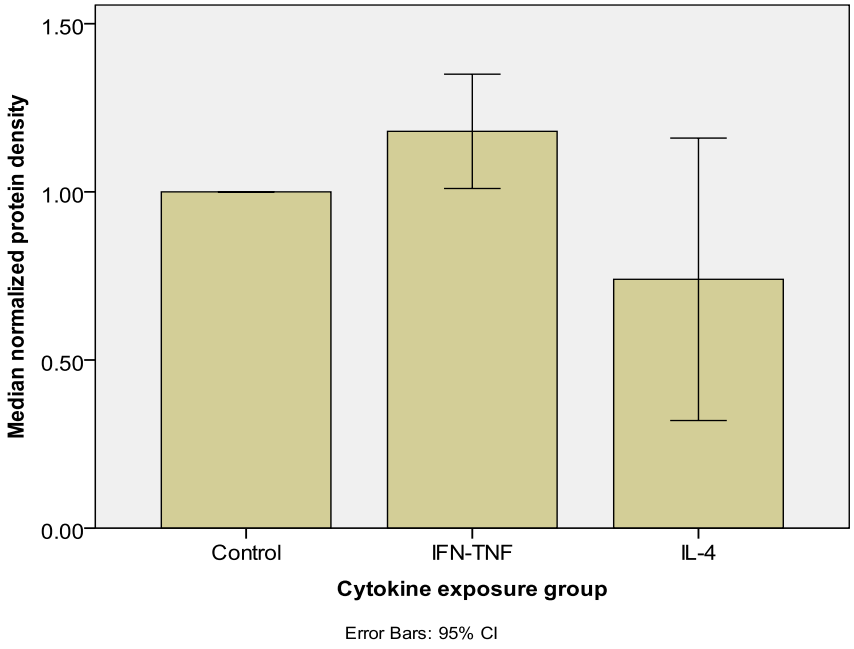

N = 2 experiments

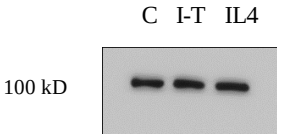

(f) Controls

Protein loading control – glyceraldehyde 3-phosphate dehydrogenase (GAPDH)

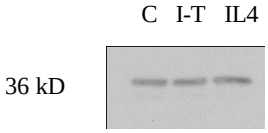

Apoptosis detection control – poly-ADP ribose polymerase (PARP) cleaved product

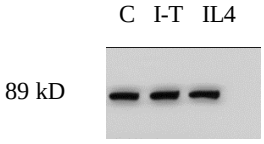

Sections a-e of this figure demonstrate combined results of Western immunoblot (graphs) for normalized protein levels at the 10 hour post-wounding time point in cytokine exposed sinonasal epithelial wound healing experiments. An example Western immunoblot is also provided for each protein in sections a-e. Section f demonstrates an example of Western immunoblot protein loading control GAPDH and apoptosis control PARP.

TABLE 4 – EPITHELIAL PROTEIN ANALYSIS FROM CONTROL AND AFRS SINONASAL TISSUE BIOPSIES

Protein	Inflammatory condition	N per group	Mean pixel density per epithelium area	Median pixel density per epithelium area	Standard deviation	95% confidence interval	Range	Mann-Whitney U test p-value
Annexin 2	Non-inflammatory AFRS	9 10	14.60 24.33	17.77 18.80	7.41 16.60	(10.01, 19.19) (14.04, 36.62)	4.50-23.71 5.56-65.98	0.221
Vinculin	Non-inflammatory AFRS	7 9	11.07 11.70	10.49 10.61	3.41 5.18	(8.71, 13.42) (8.31, 15.09)	6.24-16.94 6.14-21.69	0.874
β1-integrin	Non-inflammatory AFRS	9 10	28.18 25.14	27.49 23.41	13.12 12.03	(20.05, 36.31) (17.69, 32.59)	13.94-58.50 10.21-54.51	0.568
E-cadherin	Non-inflammatory AFRS	9 10	15.11 14.05	14.41 13.33	8.00 5.75	(10.15, 20.07) (10.49, 17.61)	7.66-34.62 5.08-26.63	0.870
β-catenin	Non-inflammatory AFRS	8 10	17.03 12.61	15.81 10.34	6.44 6.21	(12.82, 21.24) (8.76, 16.46)	6.16-23.87 6.55-23.38	0.183

This table demonstrates the numerical results of the pixel intensity analyses on sinonasal tissue biopsies from non-inflammatory control and Th2-predominant AFRS participants. There were no significant differences in pixel intensity between non-inflammatory and AFRS participant samples for any of the proteins assessed.

FIGURE 10 – GRAPHICAL REPRESENTATION OF EPITHELIAL PROTEIN ANALYSIS FROM CONTROL AND AFRS SINONASAL TISSUE BIOPSIES

(a) Annexin 2

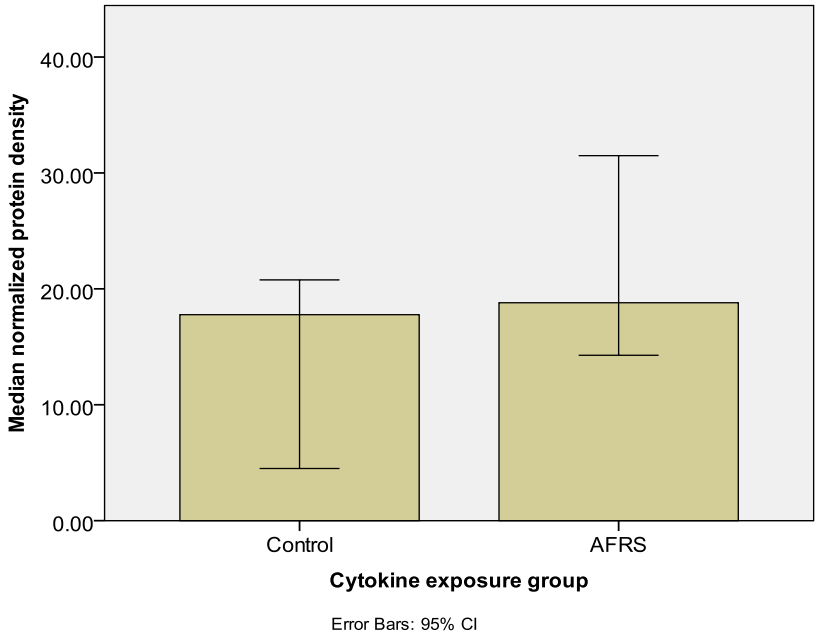

Control: N = 9
AFRS: N = 10

p = 0.221

(b) Vinculin

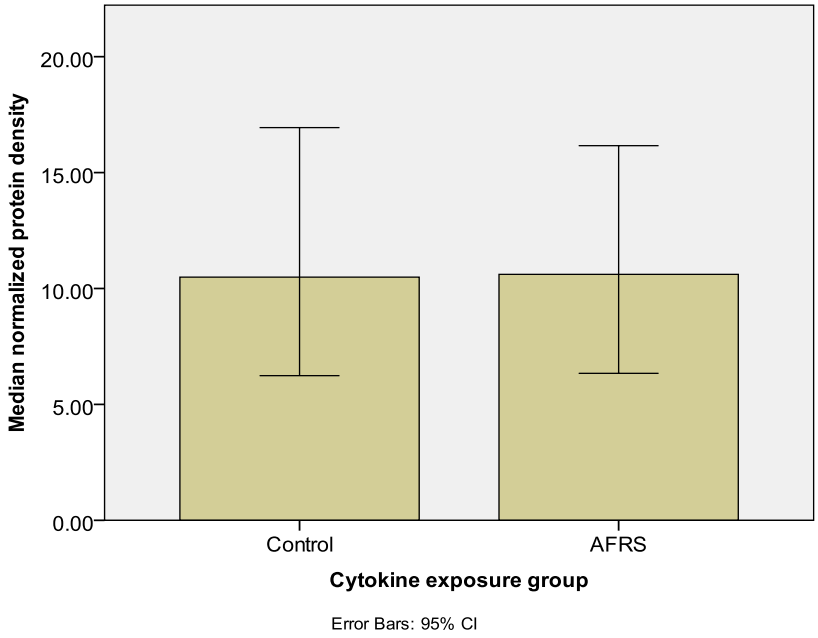

Control: N = 7
AFRS: N = 9

p = 0.874

(c) β1-integrin

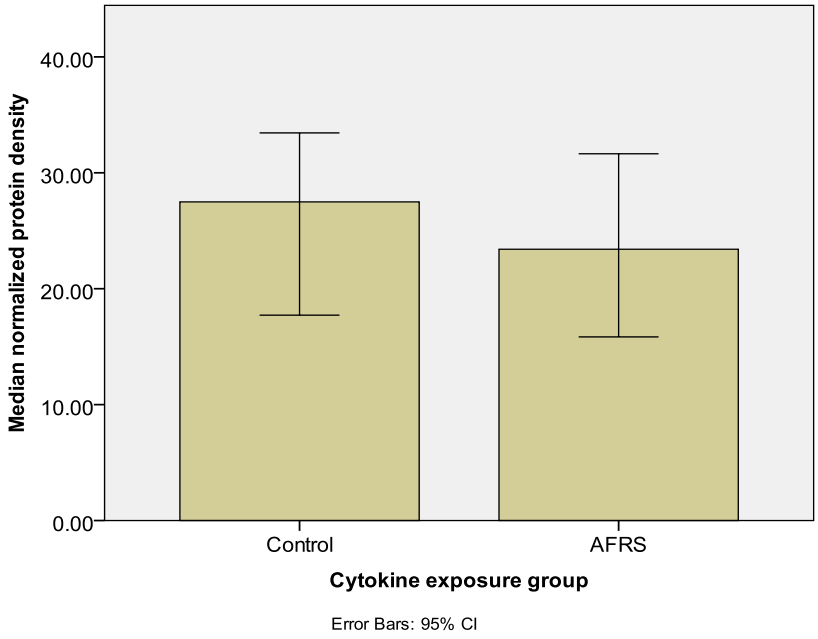

Control: N = 9
AFRS: N = 10

p = 0.568

(d) E-cadherin

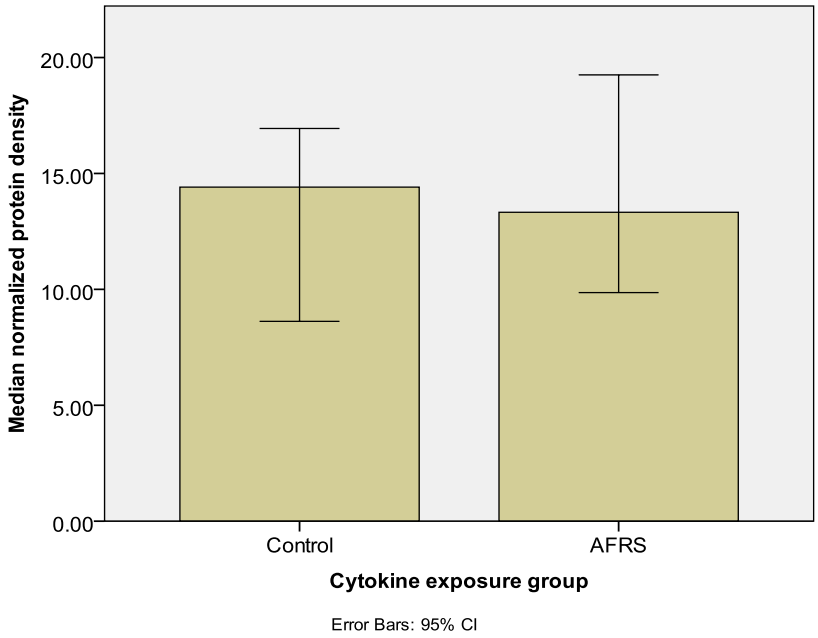

Control: N = 9
AFRS: N = 10

p = 0.870

(e) β-catenin

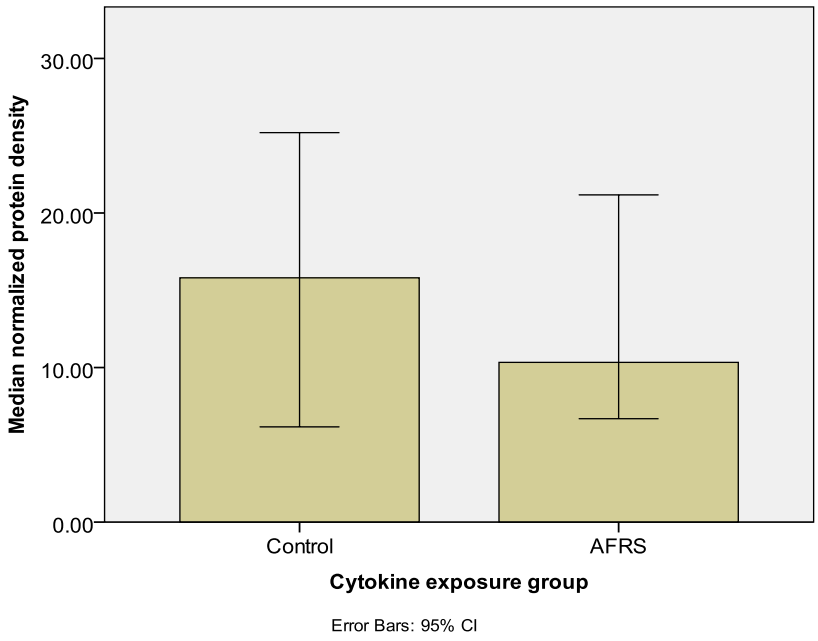

Control: N = 8
AFRS: N = 10

p = 0.183

This series of graphs depicts the results of epithelial pixel intensity analysis from sinonasal tissue biopsies in control and Th2-predominant AFRS patients. Bars represent median values, and error range represents 95% confidence intervals. None of the proteins studied had statistically significant differences between control and AFRS groups, indicating that baseline protein differences during the resting state (without epithelial migration during wound closure) are unlikely.

FIGURE 11 – EXAMPLE IMAGES OF IMMUNOFLUORESCENT PROTEIN STAINING FOR EPITHELIAL PIXEL INTENSITY ANALYSIS OF CONTROL AND AFRS SINONASAL TISSUE BIOPSIES

Annexin 2

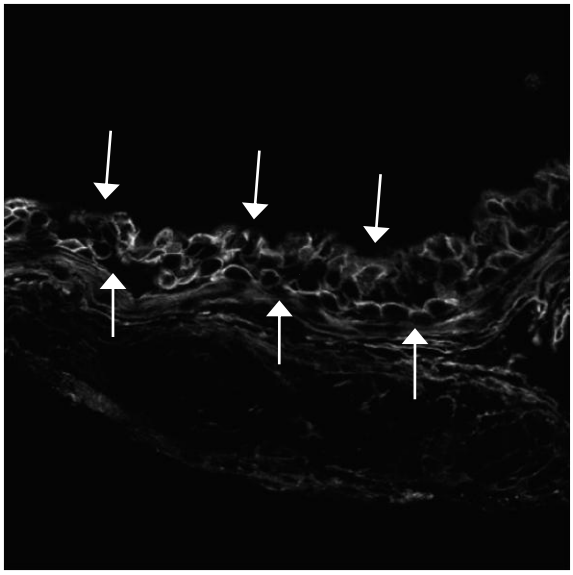

Control

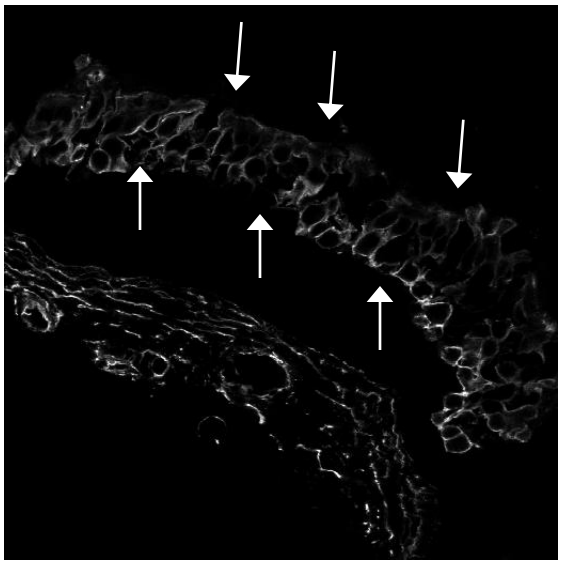

Control

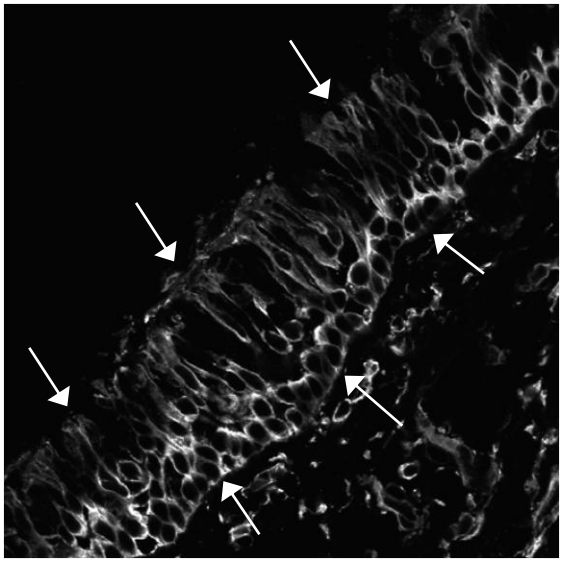

AFRS

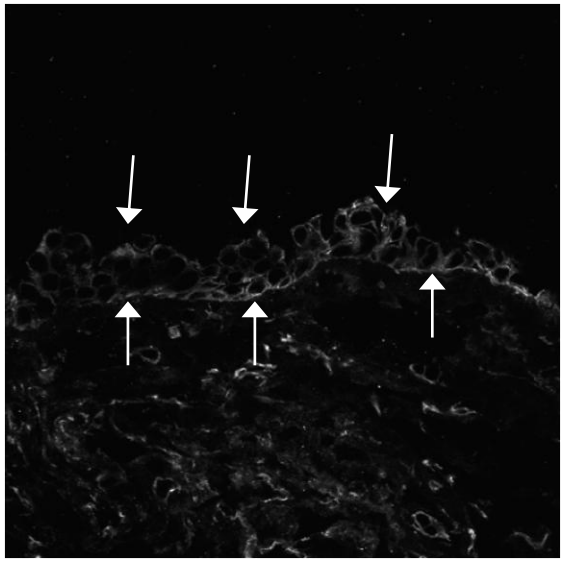

AFRS

Vinculin

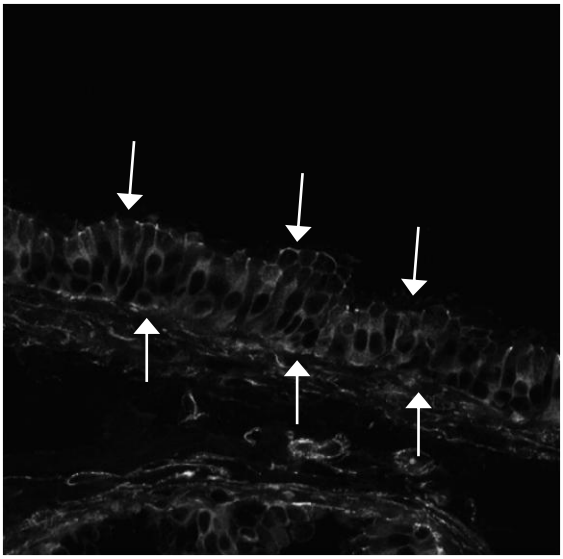

Control

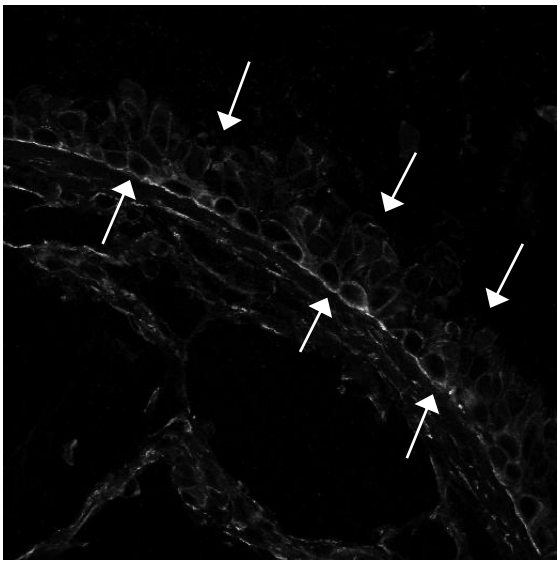

Control

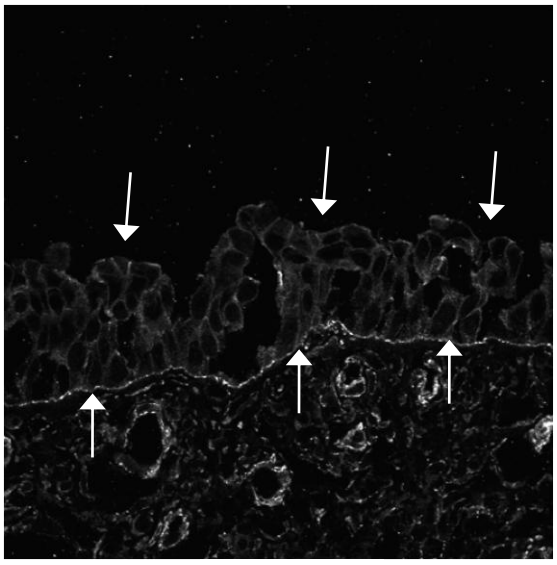

AFRS

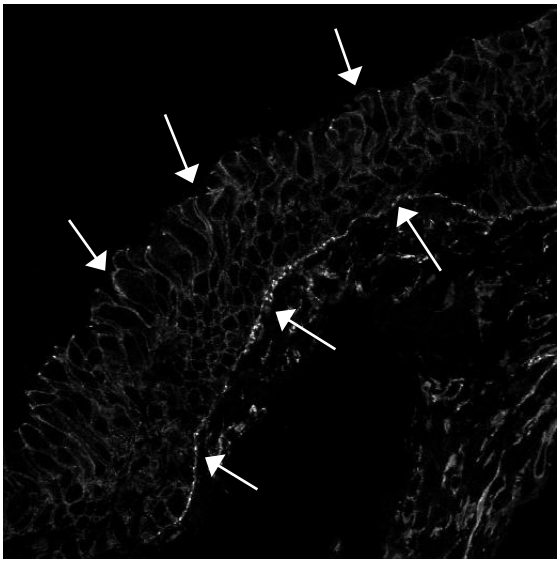

AFRS

E-cadherin

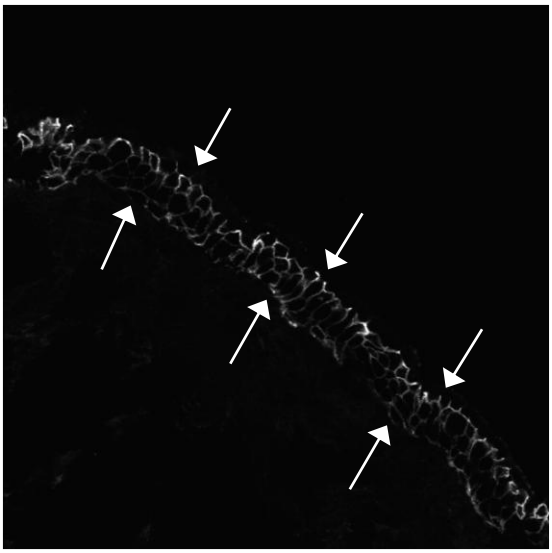

Control

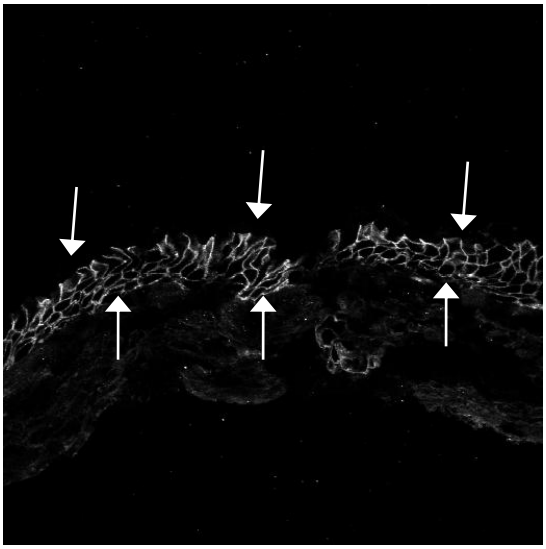

Control

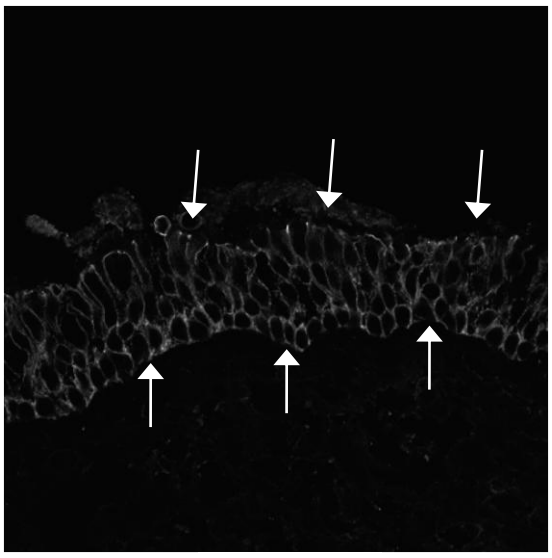

AFRS

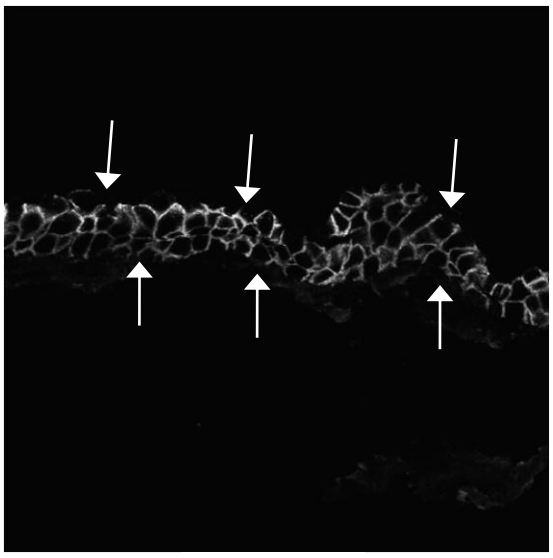

AFRS

These example images demonstrate immunofluorescent staining for epithelial migratory and adherens junction proteins assessed in control and AFRS sinonasal tissue biopsies. The epithelium is denoted by arrows. Of note, sinonasal epithelium may range from a single layer of epithelial cells to a pseudostratified columnar epithelium. In these images, it can be noted that epithelial width and protein staining intensity is rather variable. The variability in pixel intensity is also evident in the data analysis from these images. All microscopic photographs are taken at 40X magnification.

FIGURE 12 – EXAMPLE PROTEIN DENSITY GRAPHS FROM SINONASAL BIOPSY WESTERN IMMUNOBLOT ANALYSIS

(a) Annexin 2

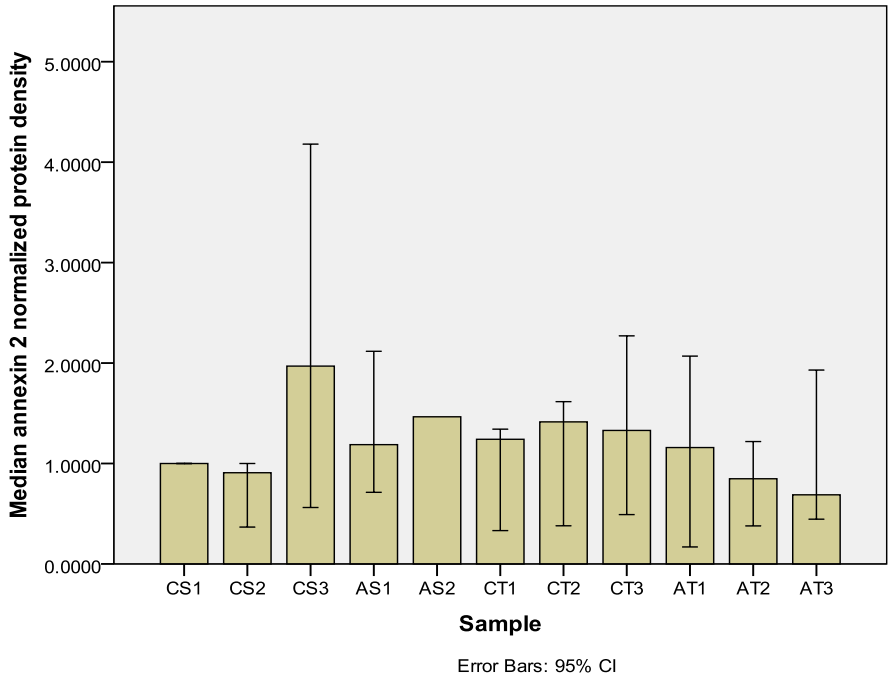

(b) Vinculin

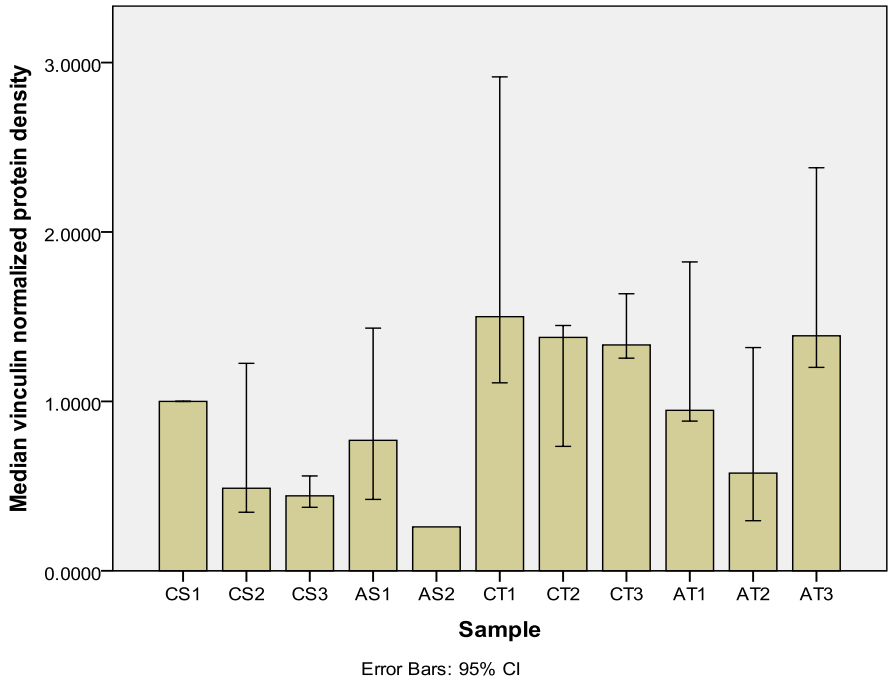

Graphs a and b demonstrate combined results from Western immunoblot analysis of sinonasal tissue biopsy baseline protein levels across 3 experimental trials. Control (C) and AFRS (A) derived specimens do not appear to have any visibly discernable differences at baseline. These results support the baseline protein immunofluorescence pixel density analysis in that no discernable epithelial migratory (annexin 2 or vinculin) differences are apparent at baseline.